Supplementary Material

Cobalt Coordination Networks Based on the Linker (Phenazine-5,10-diyl)di- and tetrabenzoate

Annette Vollrath, Xiang Liu, Nikolas Jansen, Philipp Seiffert, David Geller and Christoph Janiak *

Institut für Anorganische Chemie und Strukturchemie, Heinrich-Heine-Universität 40204 Düsseldorf, Germany

* *Correspondence: janiak@uni-duesseldorf.de*

Emails: annette.vollrath@hhu.de, xiang.liu@hhu.de, nijan113@hhu.de, philipp.seiffert@uni-duesseldorf.de, david.geller@hhu.de, janiak@uni-duesseldorf.de

Content

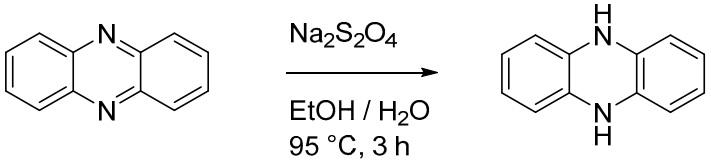
Section S1 Chemicals used 2
Section S2 Reaction schemes for ligand syntheses (Scheme S1-S5) 3
Section S3 NMR spectra 5
Section S4 IR spectra 14
Section S5 Overview of the conducted studies 16
Section S6 Crystal photographs and crystal structure images 20
Section S7 PXRD 22
Section S8 Thermogravimetric analyses 24
Section S9 Supramolecular analyses 27
Section S10 Electrochemical measurements 34

Section S1 Chemicals used

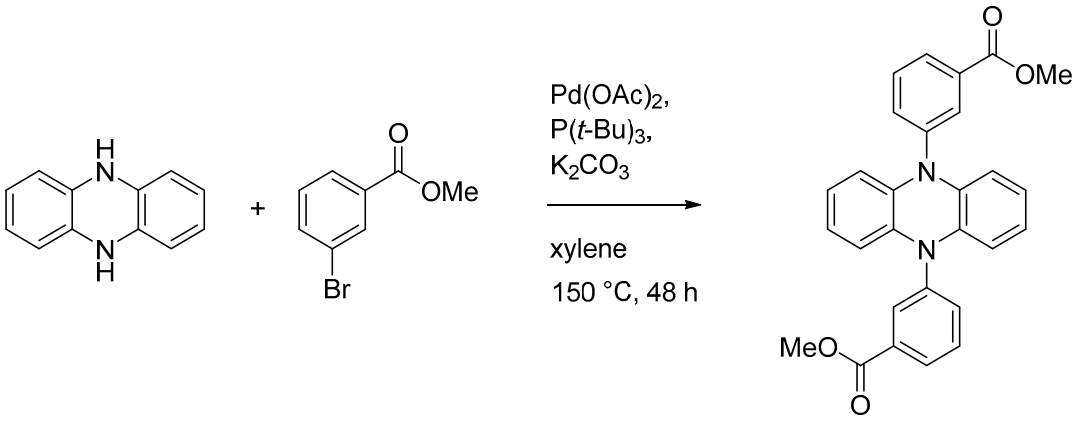
Table S1. List of chemicals used.

Chemical	Purity [%]	Supplier
Cobalt(II) nitrate hexahydrate	≥ 98	Carl Roth
Dimethyl-5-Iodoisophthalate	98.45	BLDpharm
Hydrochloric acid	37	VWR Chemicals
Lithium hydroxide monohydrate	p.a.	AppliChem
Magnesium sulfate	99.0	VWR Chemicals
Methyl-3-bromobenzoate	97	BLDpharm
Palladium(II) acetate	99.9	BLDpharm
Phenazine	99.87	BLDpharm
Potassium carbonate	99.5	Grüssing
Sodium dithionite	85	Acros Organics
Tri-*tert*-butyl-phosphine	98	Merck
1,4-Dioxane	≥ 99.8	Fisher Chemical
Chloroform	≥ 99	Fisher Chemical
Dichlormethane (DCM)	99.8	Fisher Chemical
Ethanol	≥ 99.8	Honeywell
n-Hexane	≥ 95	Sigma Aldrich
N,N-Dimethylformamide (DMF)	≥ 99.5	Fisher Chemical
Xylene (isomer mixture)	98.7	VWR Chemicals

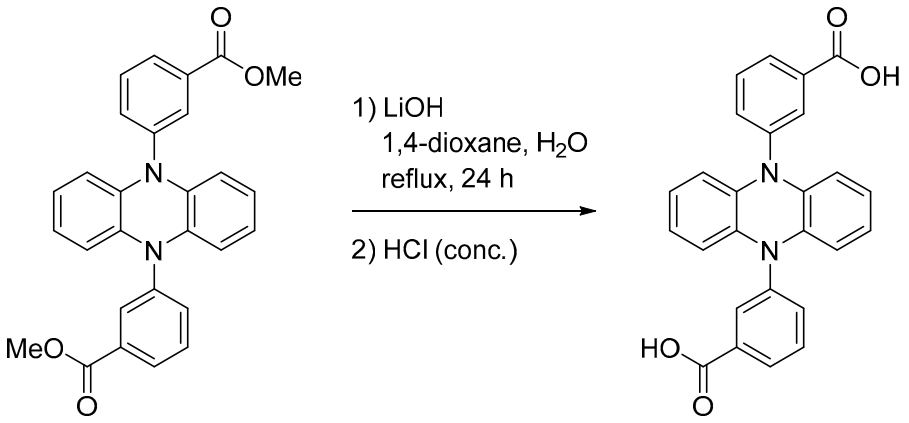
Section S2 Reaction schemes for ligand syntheses (Scheme S1-S5)



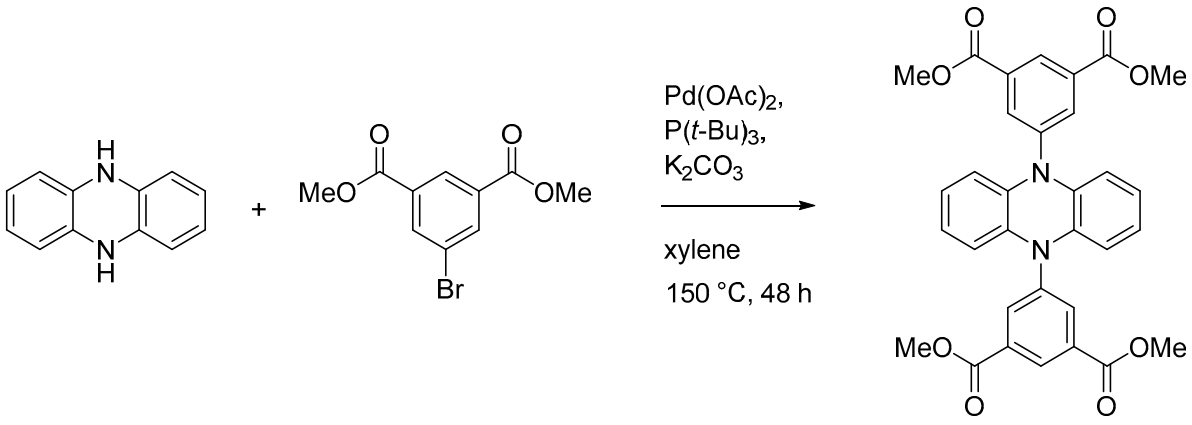
Scheme S1. Synthesis of 5,10-dihydrophenazine.



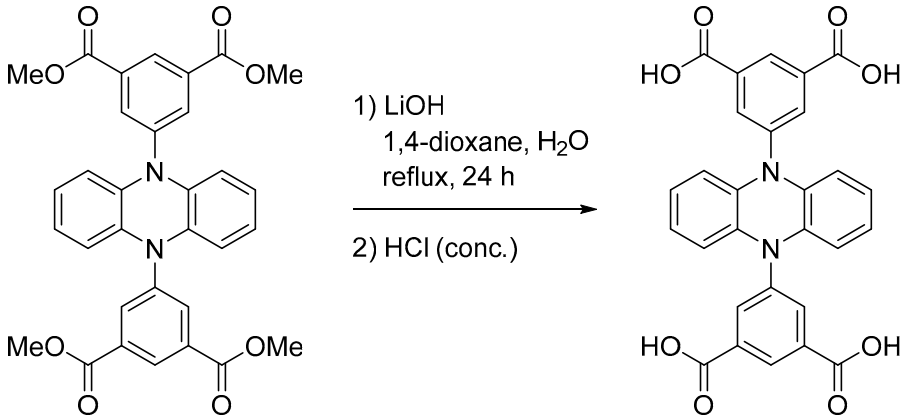
Scheme S2. Synthesis of dimethyl-3,3'-(phenazine-5,10-diyl)dibenzoate.



Scheme S3. Synthesis of 3,3'-(phenazine-5,10-diyl)dibenzoic acid (H_2pdb).



Scheme S4. Synthesis of tetramethyl-5,5'-(phenazine-5,10-diyl)diisophthalate.



Scheme S5. Synthesis of 5,5'-(phenazine-5,10-diyl)diisophthalic acid (H_4pdi).

Section S3 NMR spectra

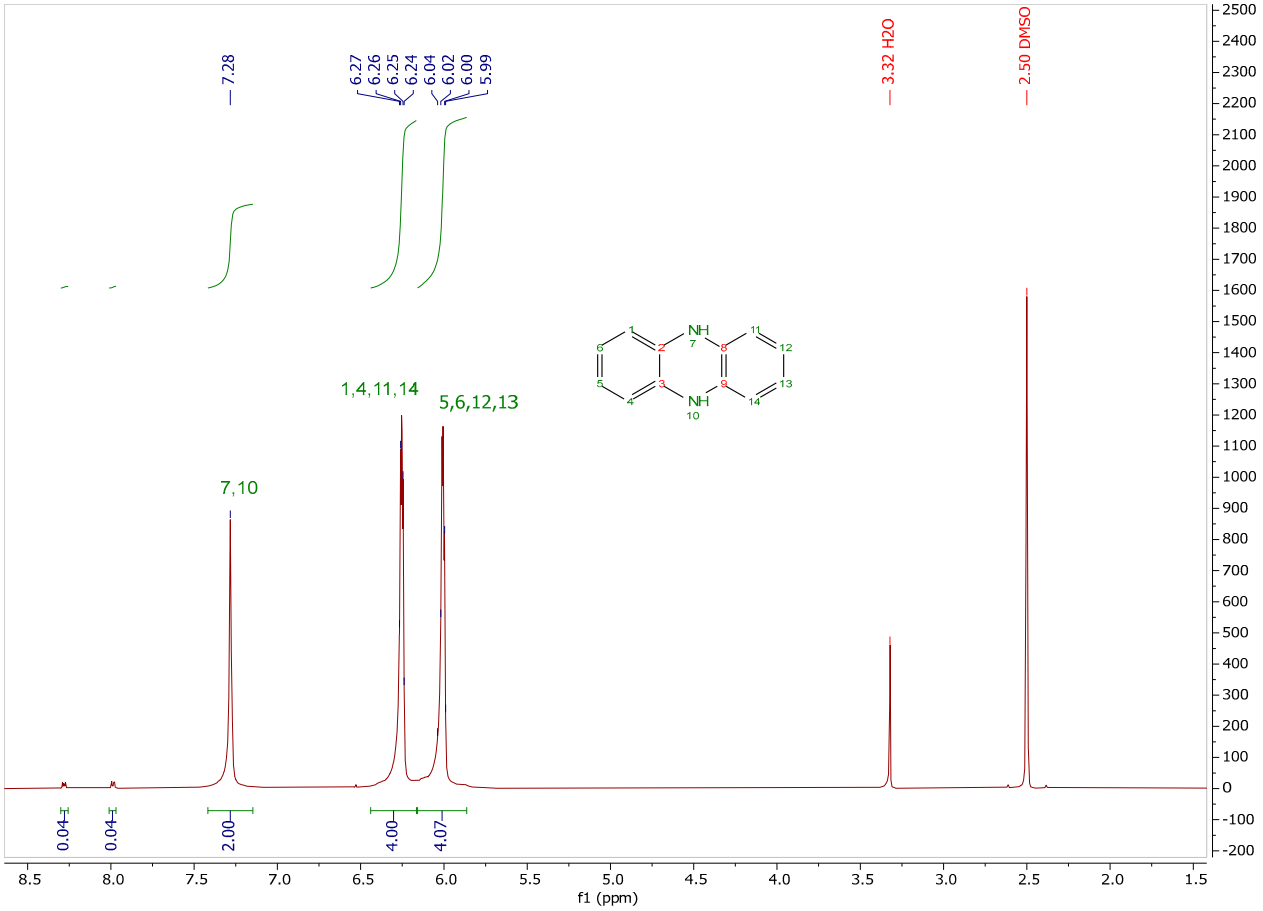


Figure S1. ^{1}H-NMR-spectrum of 5,10-dihydrophenazin (300 MHz, DMSO-d_6).
The two doublets at 6.01 ppm and 6.26 ppm can be attributed to the two benzene rings in 5,10-dihydrophenazine, while the singlet at 7.29 ppm can be assigned to the NH protons. At 8.00 ppm and 8.30 ppm, there are two further signals that can be assigned to the remaining or re-oxidized phenazine starting material. The percentage content of phenazine in the sample can be calculated from the ratios of the signals of the reactant to the product as 1%.

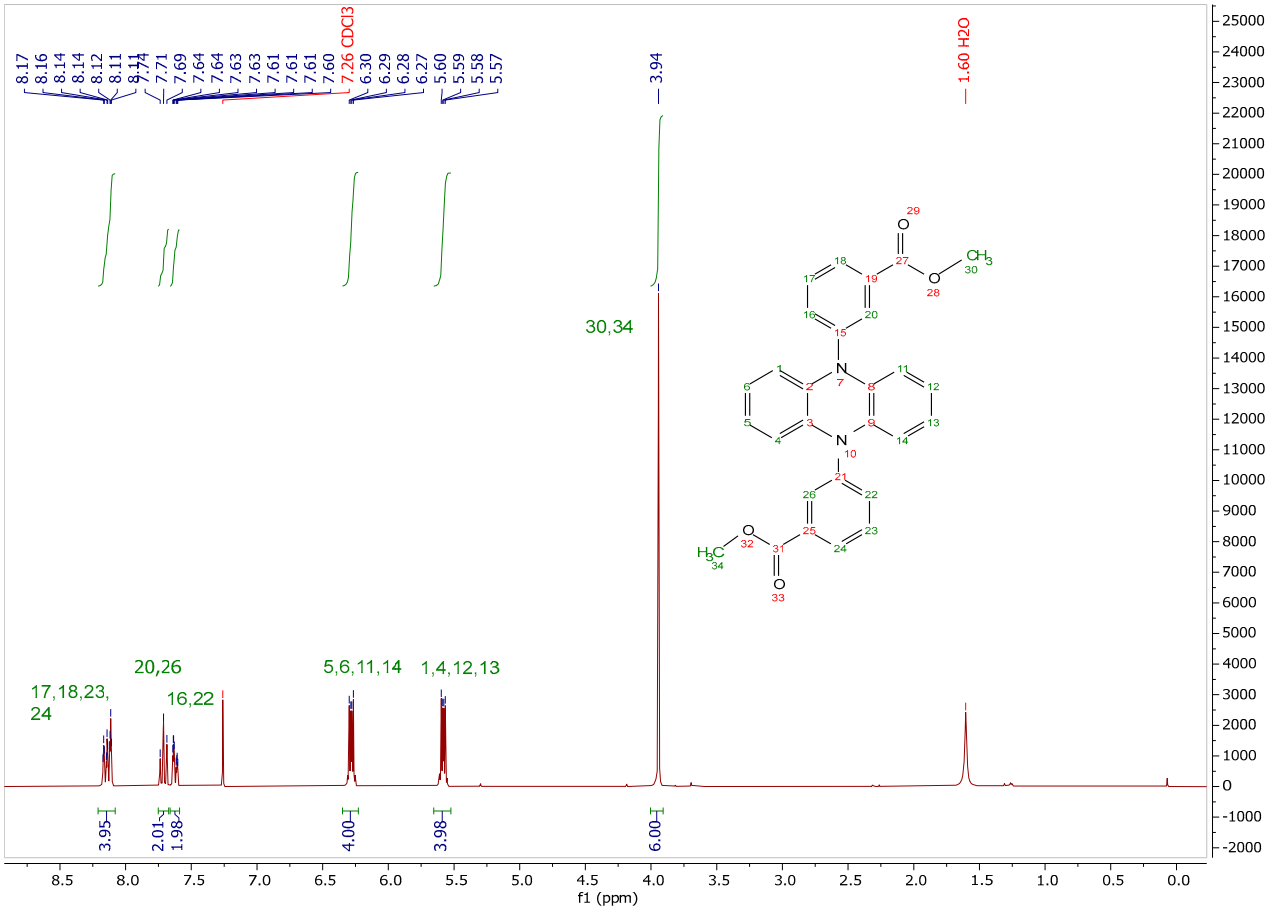


Figure S2. ^{1}H-NMR-spectrum of dimethyl-3,3'-(phenazine-5,10-diyl)dibenzoate (H_2pdb) (300 MHz, $CDCl_3$). In the ^{1}H NMR spectrum, the singlet at 3.94 ppm can be assigned to the two methyl groups in dimethyl-3,3'-(phenazine-5,10-diyl)dibenzoate, while the doublet at 5.58 ppm and 6.28 ppm can be assigned to the protons in the 5,10-dihydrophenazine core. The multiplet from 7.59 ppm to 7.65 ppm can be assigned to the protons at positions 20 and 25 of the benzenoate ring and the triplet at 7.71 ppm belongs to the protons at positions 21 and 26. The multiplet from 8.08 ppm to 8.20 ppm can be assigned to the other four protons on the benzoate ring. In addition, a small water signal at 1.60 ppm is observed, which may originate from the water in the sample and the water contained in the solvent.

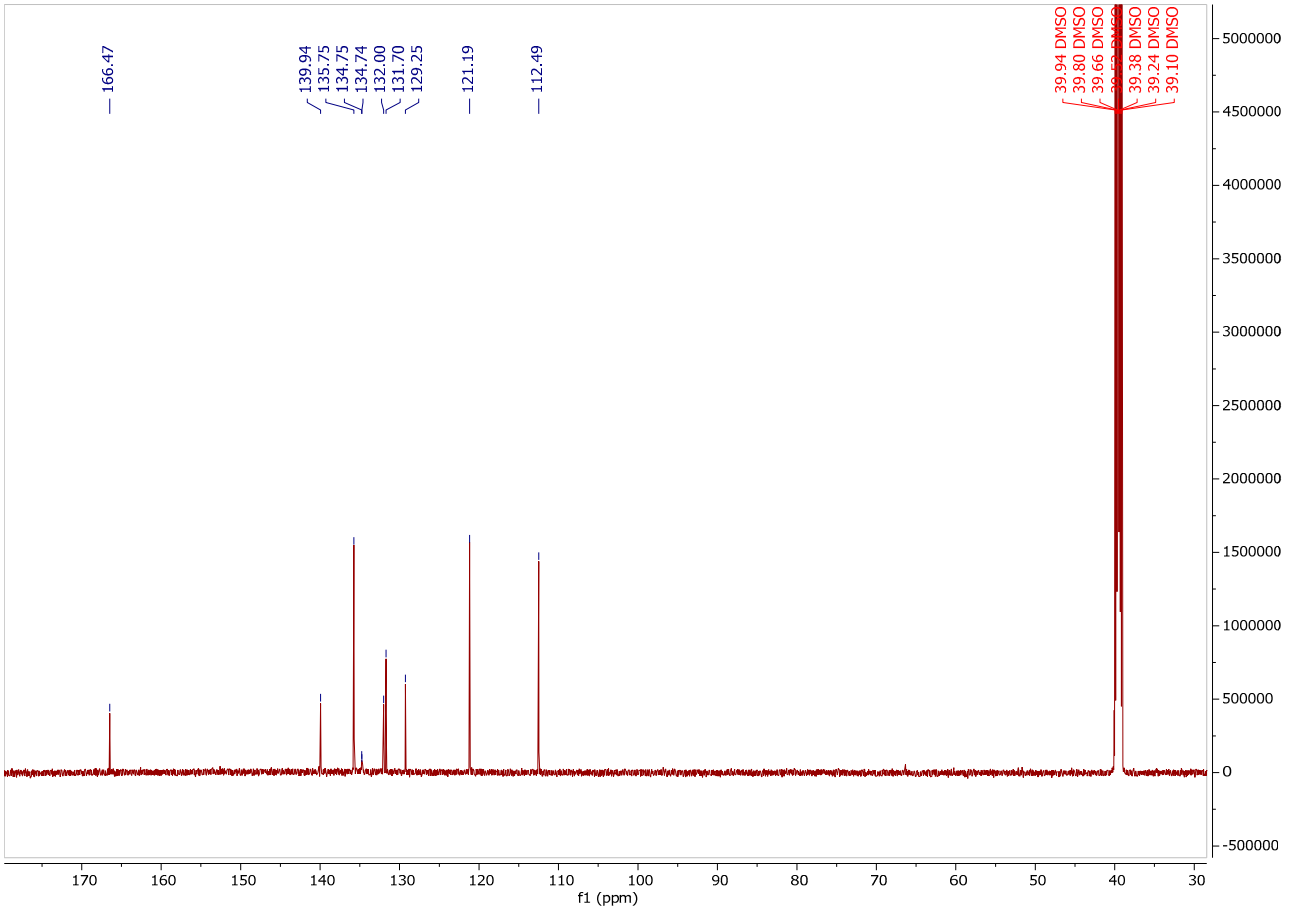


Figure S3. $^{13}C\{1H\}$-NMR-spectrum of dimethyl-3,3'-(phenazine-5,10-diyl)dibenzoate (600 MHz, $CDCl_3$).

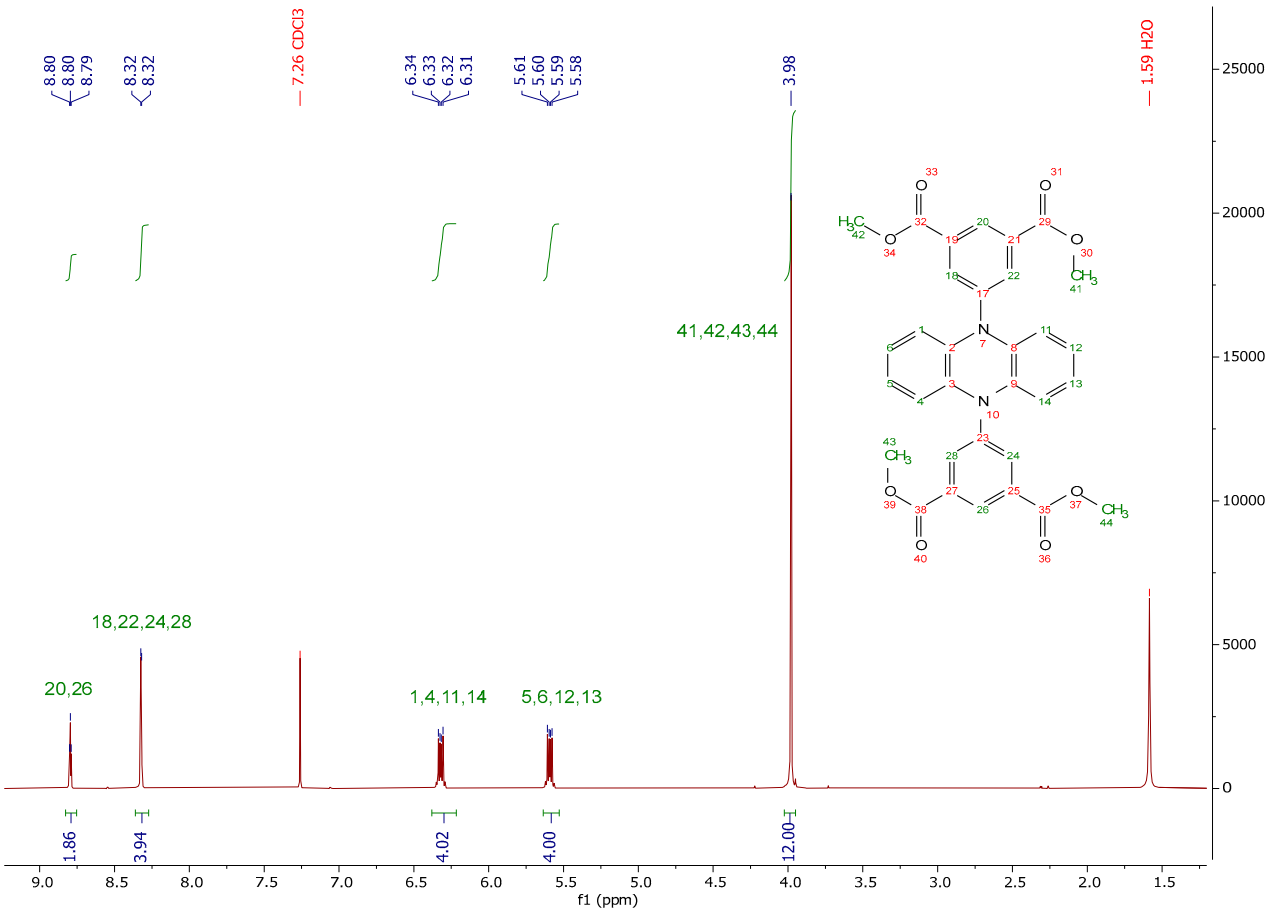


Figure S4. ^{1}H-NMR-spectrum von tetramethyl-5,5'-(phenazine-5,10-diyl)diisophthalate (300MHz, $CDCl_3$). All five chemically different signals were observed in the ^{1}H NMR spectrum. The singlet located at 3.98 ppm can be assigned to the four methyl groups, while the two doublets of doublets at 5.59 and 6.32 ppm can be assigned to the protons of the 5,10-dihydrophenazine core of this molecule. The two signals between 8.0 ppm and 9.0 ppm belong to the three protons of the isophthalate benzene rings.

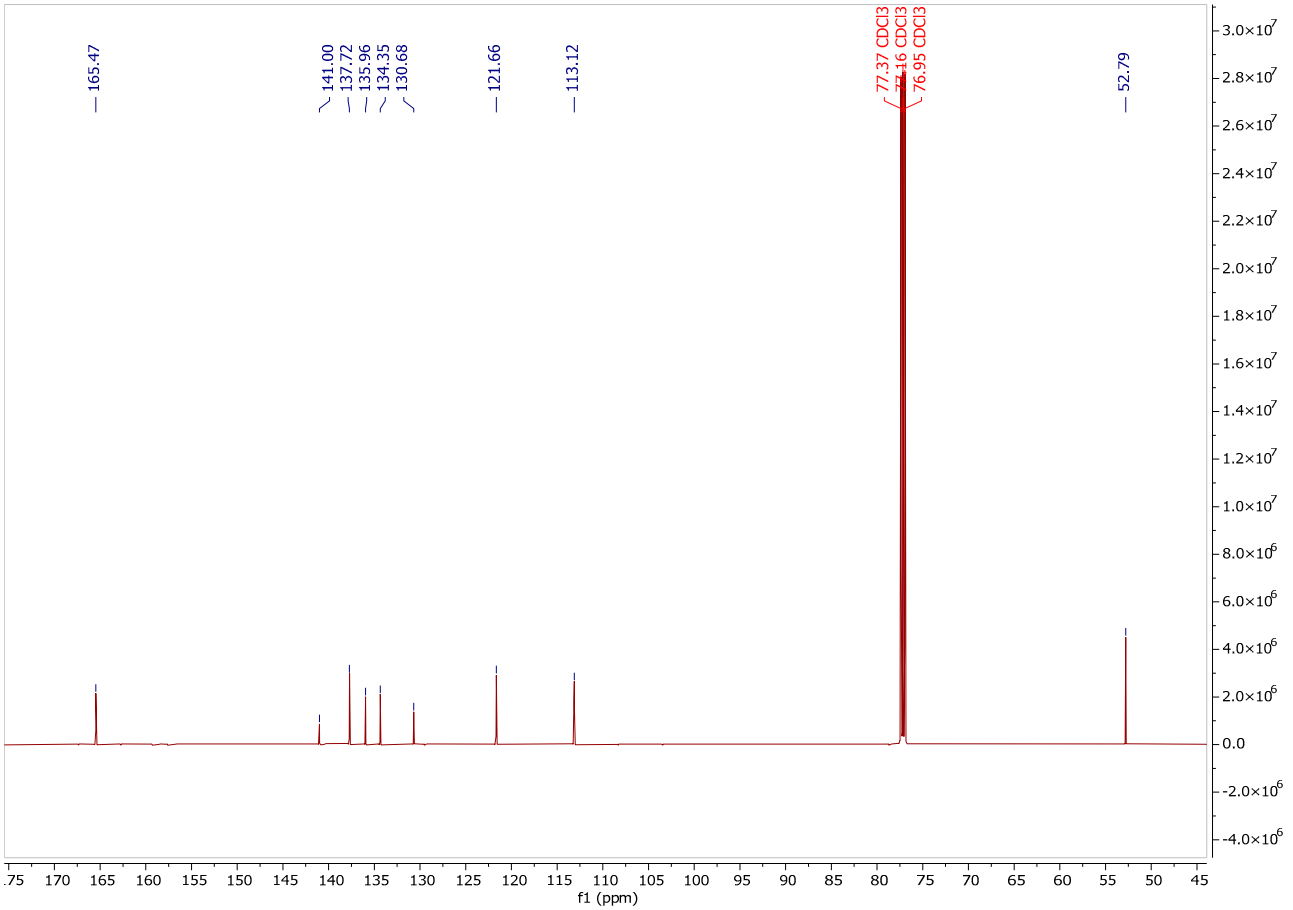


Figure S5. $^{13}C\{1H\}$-NMR-spectrum von tetramethyl-5,5'-(phenazine-5,10-diyl)diisophthalate (600MHz, $CDCl_3$).

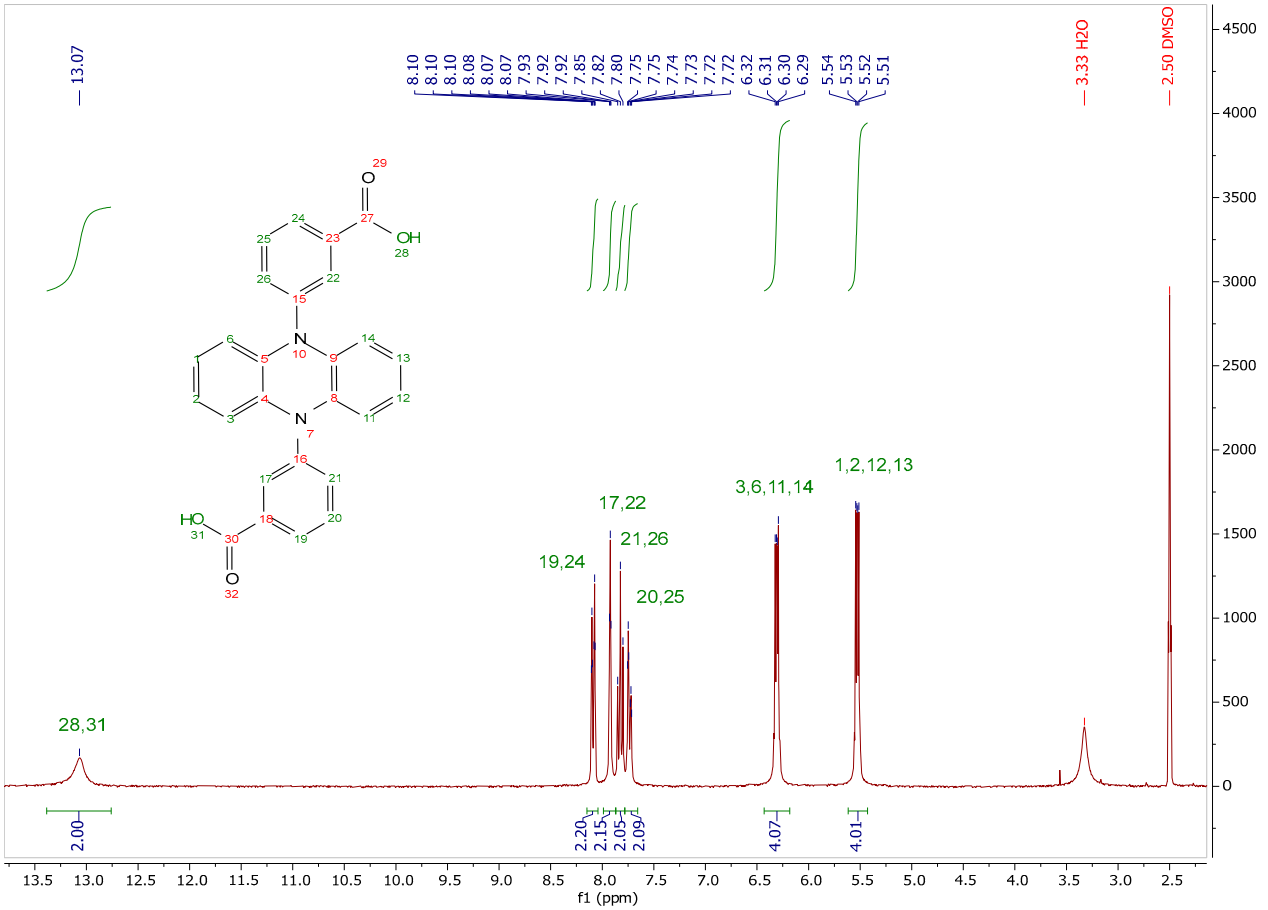


Figure S6. ^{1}H-NMR-spectrum of 3,3'-(phenazine-5,10-diyl)dibenzoic acid (H_2pdb) (300 MHz, DMSO-d_6). The two doublets at 5.52 ppm and 6.30 ppm can be assigned to the protons on the two anellated benzene rings of the 5,10-dihydrophenazine core. The four signals between 7.60 ppm and 8.20 ppm can be assigned to the protons on the two benzoate rings. The integrals in the spectrum correspond exactly to the expected number of hydrogen atoms.

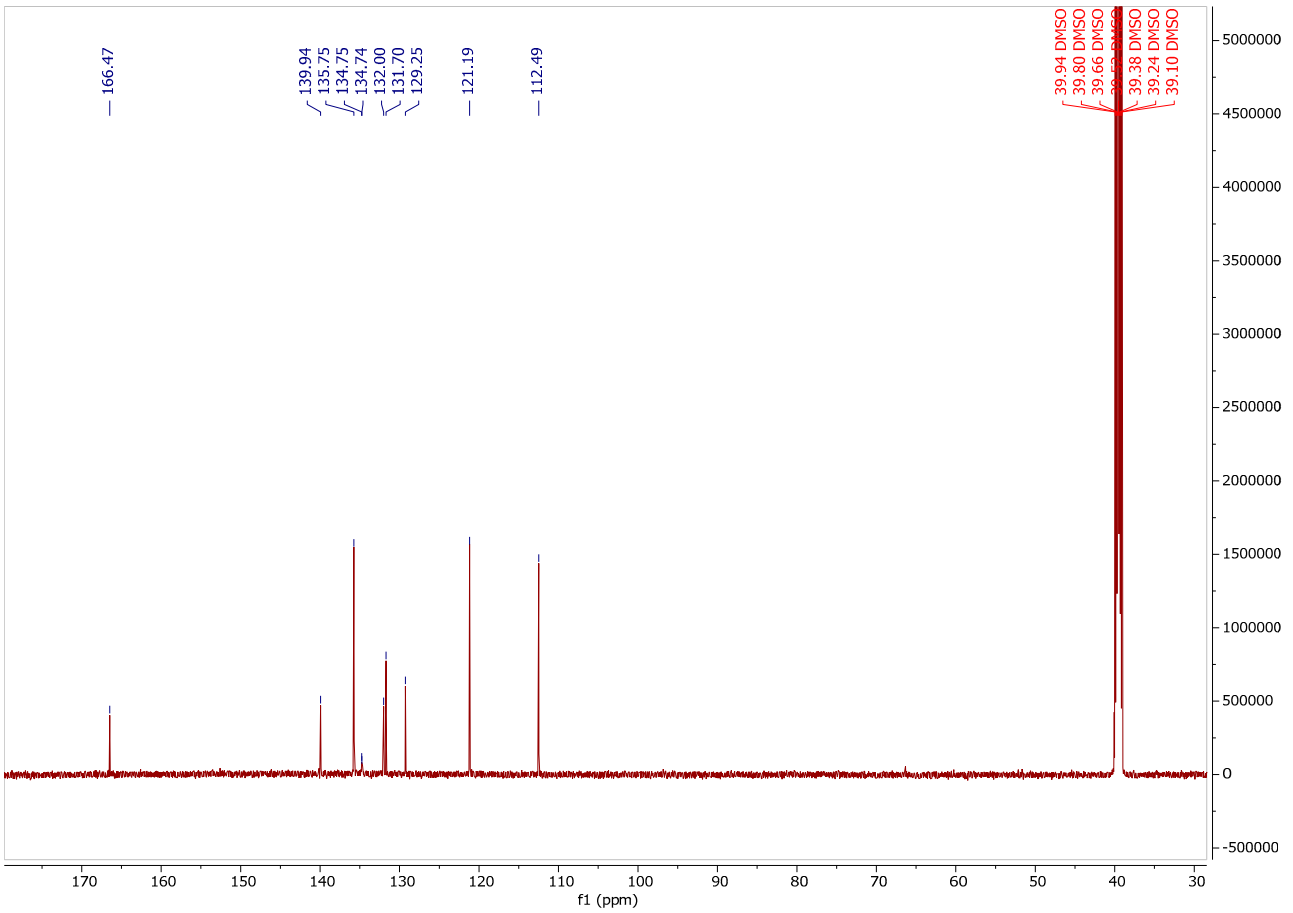


Figure S7. $^{13}C\{^{1}H\}$-NMR-spectrum of 3,3'-(phenazine-5,10-diyl)dibenzoic acid (H_2pdb) (600 MHz, DMSO-d_6).

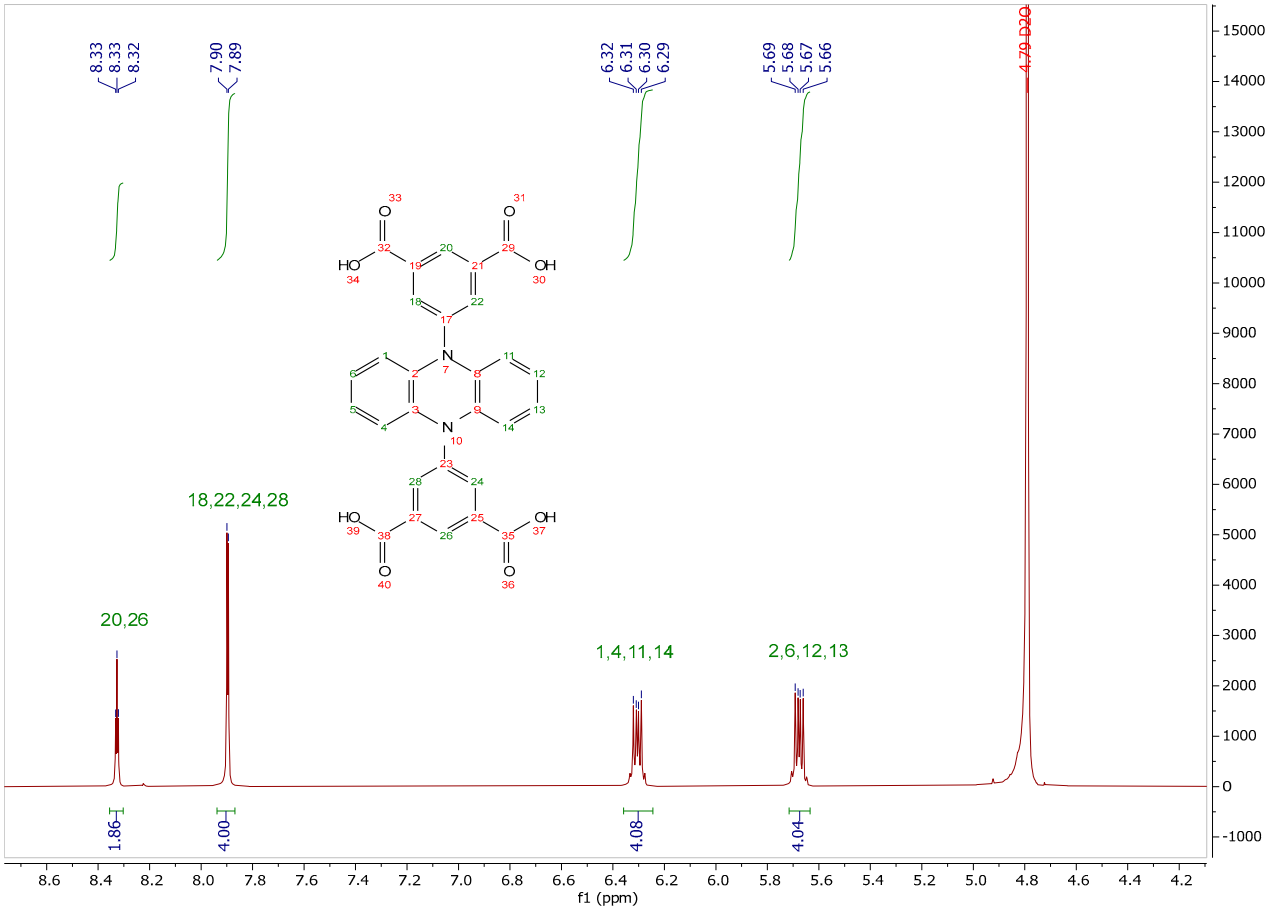


Figure S8. ^{1}H-NMR-Spectrum of 5,5'-(phenazine-5,10-diyl)diisophthalic acid (H_4pdi) (300 MHz, D_2O). The two doublets at 5.81 ppm and 6.44 ppm can be assigned to the 5.10-dihydrophenazine core, the two signals between 8.0 ppm and 8.5 ppm to the protons on the two isophthalate rings. The integrals correspond to the number of protons in the molecule.

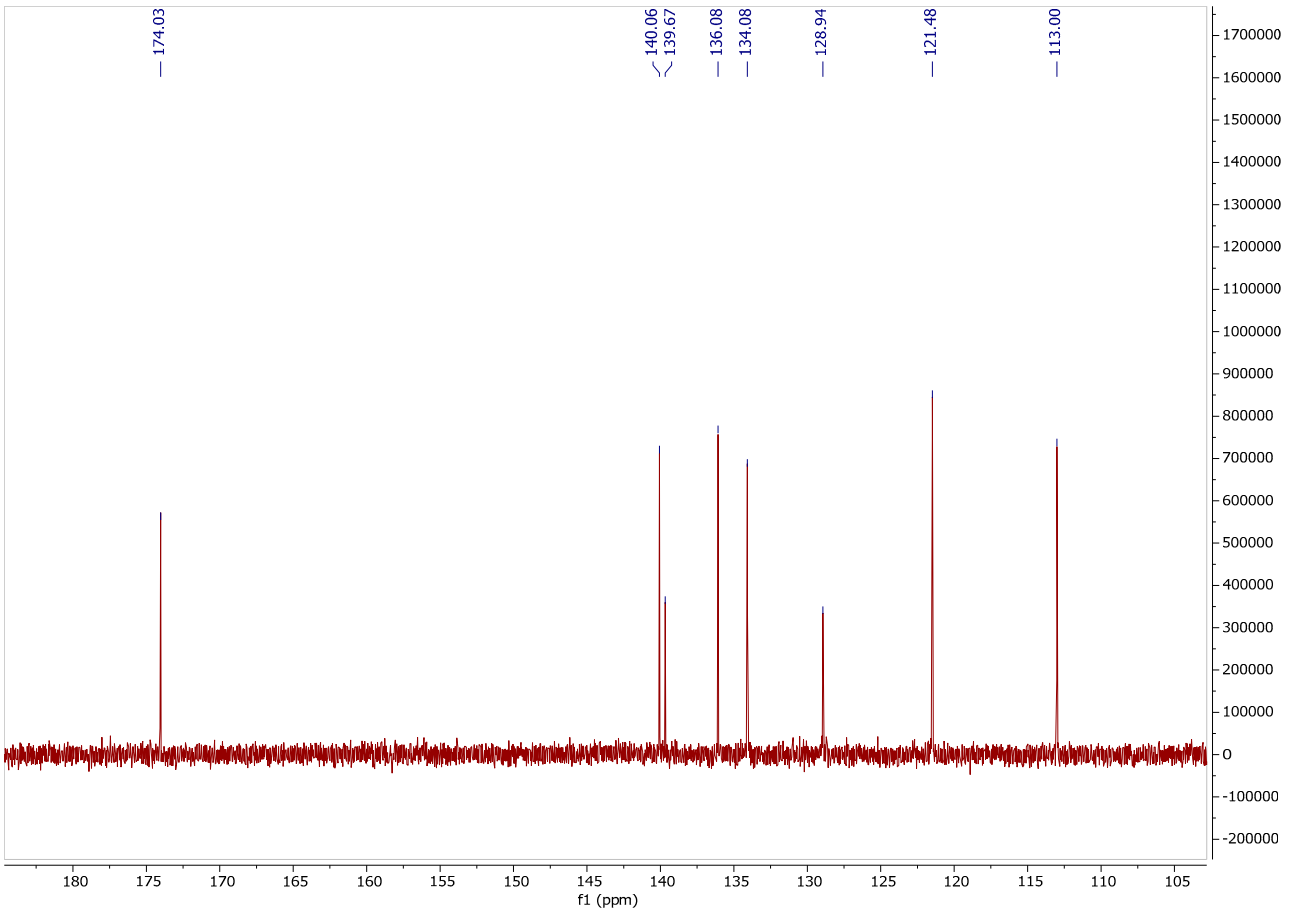


Figure S9. $^{13}C\{^{1}H\}$-NMR-Spectrum of 5,5'-(phenazine-5,10-diyl)diisophthalic acid (H_4pdi) (600 MHz, D_2O).

Section S4 IR spectra

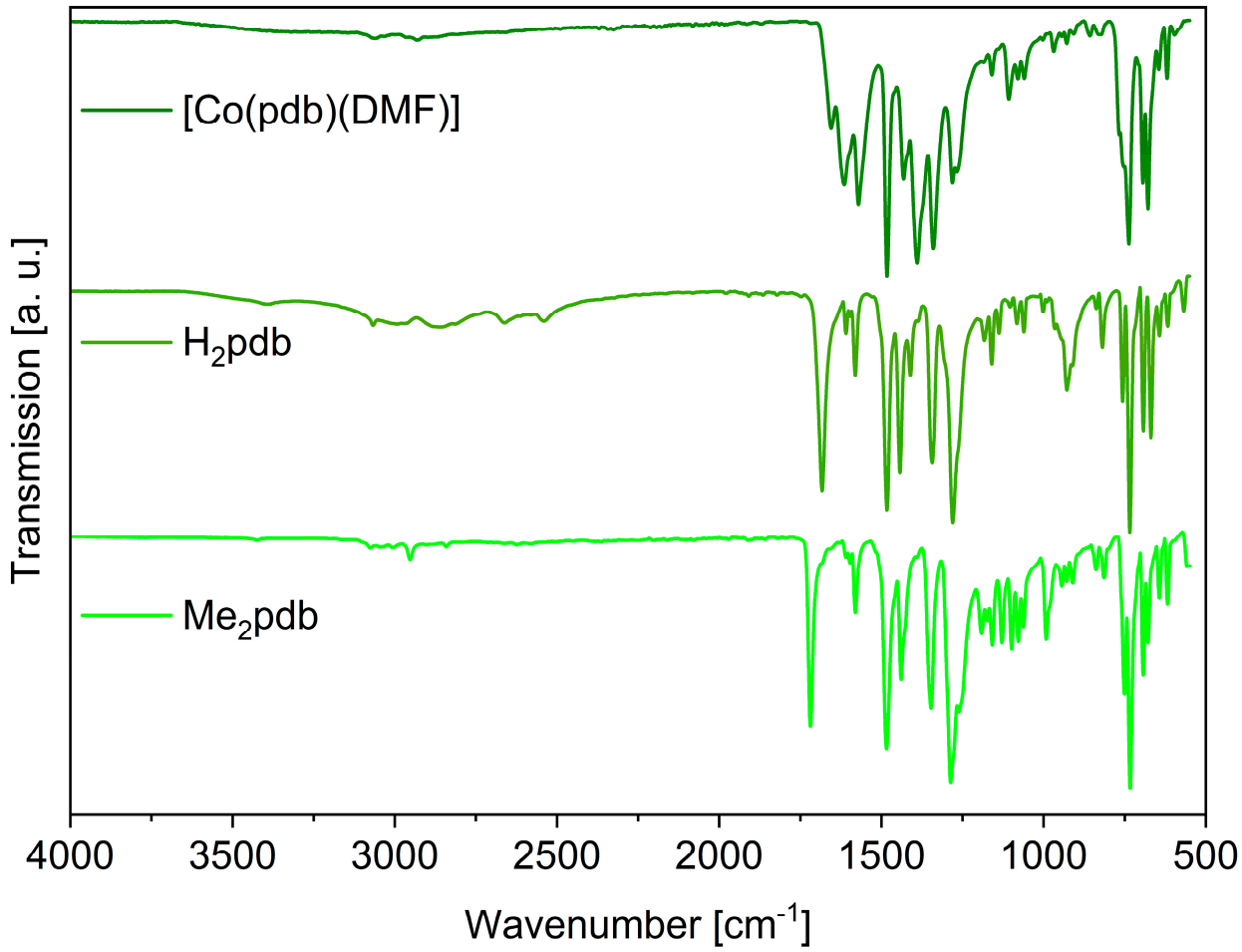


Figure S10. IR spectra of [Co(pdb)(DMF)] (dark green), of 3,3'-(phenazine-5,10-diyl)dibenzoic acid (H_2pdb, olive green) and dimethyl-3,3'-(phenazine-5,10-diyl)dibenzoate (Me_2pdb, light green).

In the spectrum of the coordination polymer, no absorption band corresponding to the O–H stretching vibration is observed in the range between 2400 and 3200 cm^{-1}, which is clearly present in the spectrum of the dibenzoic acid linker H_2pdb and absent in the spectrum of the corresponding methyl ester Me_2pdb. This indicates deprotonation of the carboxylic acid groups upon coordination to the cobalt centers. The C=O stretching vibration of the carboxylic acid group is observed in the H_2pdb linker spectrum at 1682 cm^{-1}, while the ester C=O stretching vibration in Me_2pdb appears at a slightly higher wavenumber. In the spectrum of the coordination polymer, this band is replaced by two bands at 1655 and 1615 cm^{-1}, which can be assigned to the asymmetric and symmetric stretching vibrations of the coordinated carboxylate groups, confirming their bridging coordination mode. Additionally, an absorption band at 1483 cm^{-1} is observed in the spectra of the coordination polymer as well as in both linker compounds and can be attributed to the C=C stretching vibration of the aromatic benzene rings. The band at approximately 1280 cm^{-1}, present in all spectra, can be assigned to C–O stretching vibrations of the carboxylate or ester groups, potentially with contributions from C–N stretching modes. A strong absorption band at 1390 cm^{-1} appears in the spectrum of the coordination polymer and can be attributed to the C–N stretching vibration of coordinated DMF molecules, supporting the presence of DMF in the coordination environment of the cobalt centers.

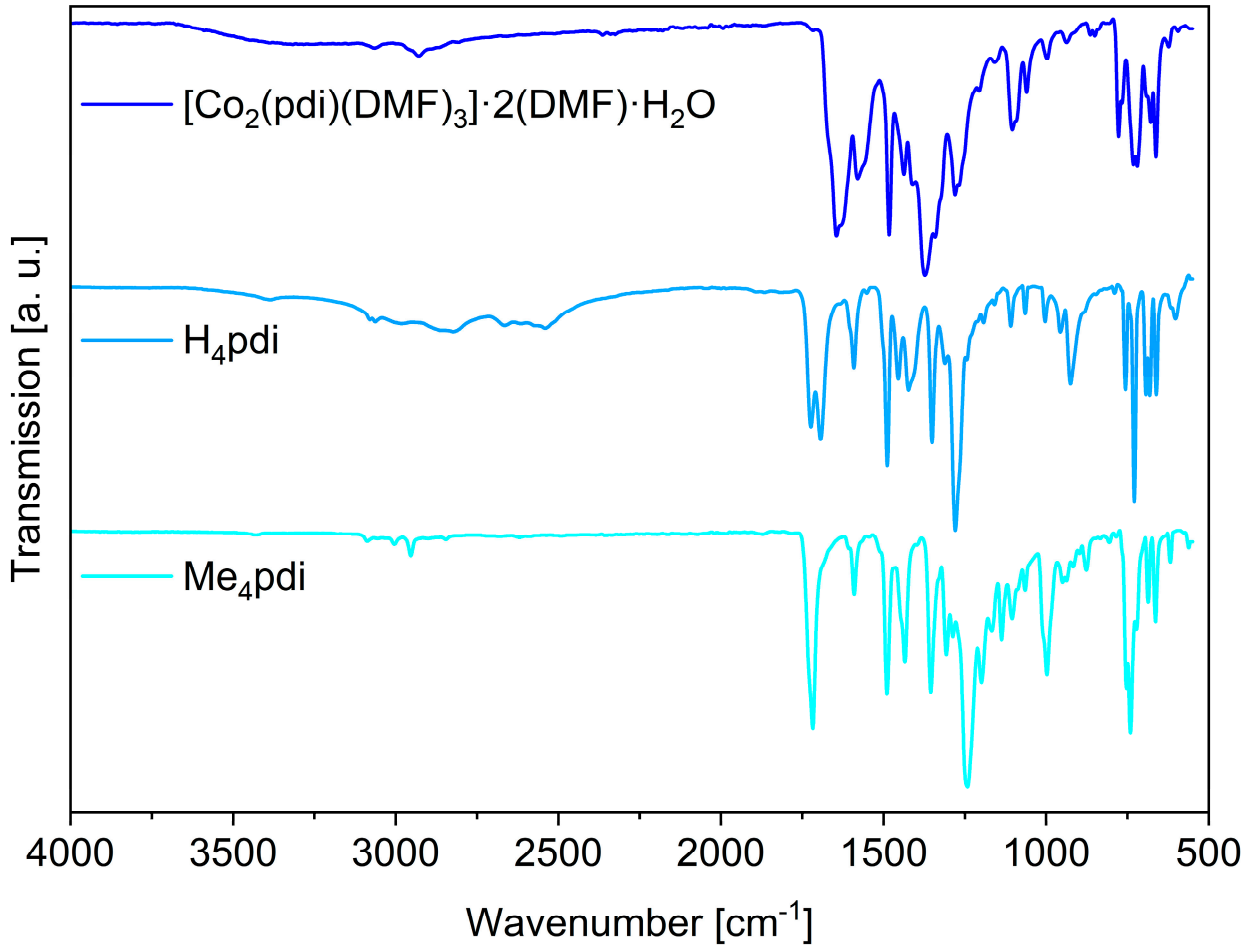


Figure S11. IR spectra of $[Co_2(pdi)(DMF)_3]\cdot 2(DMF)\cdot H_2O$ (dark blue), 5,5'-(phenazine-5,10-diyl)diisophthalic acid (H_4pdi, light blue) and tetramethyl-5,5'-(phenazine-5,10-diyl)diisophthalate (Me_4pdi, cyan).

In the spectrum of the free acid linker H_4pdi, a broad absorption band in the range between 2400 and 3300 cm^{-1} is observed, which can be assigned to the O–H stretching vibration of the carboxylic acid groups. This band is absent in the spectra of both the coordination compound and the Me_4pdi, indicating deprotonation of the carboxylic acid groups upon coordination to the cobalt centers. In the spectrum of H_4pdi, a strong band at approximately 1690 cm^{-1} is attributed to the C=O stretching vibration of the carboxylic acid groups. Upon coordination, this band is replaced by multiple bands in the range between 1650 and 1550 cm^{-1} in the spectrum of the coordination compound. These bands can be assigned to the asymmetric and symmetric stretching vibrations of coordinated carboxylate groups, consistent with their involvement in metal coordination. An absorption band around 1480 cm^{-1} is present in the spectra of the coordination compound as well as in both linker derivatives and can be attributed to the C=C stretching vibrations of the aromatic rings of the pdi linker. Additional bands observed in the region between 1300 and 1400 cm^{-1} can be assigned to C–O stretching vibrations of the carboxylate or ester groups, potentially overlapping with contributions from C–N stretching modes. Furthermore, a strong absorption band in the coordination compound around 1390 cm^{-1} can be attributed to the C–N stretching vibration of coordinated DMF molecules, confirming the presence of DMF in the coordination environment. The broad absorption observed above 3300 cm^{-1} can be assigned to O–H stretching vibrations of lattice water molecules.

Section S5 Overview of the conducted studies

Table S2. Overview of the metal salts, linkers, any additives or modulators, temperatures, metal-to-linker ratio, and results used.

Metal salt $Co(NO_3)_2 \cdot 6\ H_2O$ (giving [Co(pdb)(DMF)])								
Sample	**Metal salt [mg]**	**H_2pdb [mg]**	**DABCO [mg]**	**Acid (20 µL)**	**Temperature [°C]**	**Molar M:L ratio**	**Results**	**Yields [%]**
1	20	15			100	2:1	Dark red crystals	69
2	20	15	3.9		100	2:1	Dark red crystals	40
3	16	12			100	2:1	Dark red crystals	38
4	16	11.9			100	2:1	Dark red crystals	38
5	14.7	11			100	2:1	Dark red crystals	37
6	15.3	11.5			100	2:1	Dark red crystals	42
7	14.7	11	2.9		100	2:1	Dark red crystals	36
8	15.3	11.5		HCl	100	2:1	PXRD H_2pdb linker	-
9	15.7	11.6		TFA	100	2:1	Dark red crystals	34
10	16.1	12.1		HAc	100	2:1	Dark red crystals	42
11	18.8	14			100	2:1	Dark red crystals	49
12	15.7	11.8			100	2.1	Dark red crystals	46
13	18.8	14.1			100	2:1	Dark red crystals	48
Metal salt CoSO4·7 H_2O								
Sample	**Metal salt [mg]**	**H_2pdb [mg]**	**DABCO [mg]**	**Acid (20 µL)**	**Temperature [°C]**	**Molar M:L ratio**	**Results**	**Yields [%]**
1	3.2	10		TFA	120	1:3	PXRD H_2pdb linker	-
Metal salt $CoCl_2 \cdot 6\ H_2O$								
Sample	**Metal salt [mg]**	**H_2pdb [mg]**	**DABCO [mg]**	**Acid (20 µL)**	**Temperature [°C]**	**Molar M:L ratio**	**Results**	**Yields [%]**
1	2.7	15	1.3	HAc	100	1:3	PXRD H_2pdb linker	-
2	2.7	15		HAc	120	1:3	PXRD H_2pdb linker	-
3	2.7	15	1.3	HCl	100	1:3	PXRD H_2pdb linker	-
4	2.7	15	1.3	TFA	120	1:3	PXRD H_2pdb linker	-
5	2.7	15	1.3		120	1:3	PXRD H_2pdb linker	-
Metal salt $Co(NO_3)_2 \cdot 6\ H_2O$ (giving $[Co(pdi)(DMF)_3] \cdot 2(DMF) \cdot H_2O$)								
Sample	**Metal salt [mg]**	**H_4pdi [mg]**	**DABCO [mg]**	**Acid (20 µL)**	**Temperature [°C]**	**Molar M:L ratio**	**Results**	**Yields [%]**
1	20	15			100	2:1	Dark red crystals	62
2	20	15	3.9		100	2:1	Dark red crystals	49
3	16	12			100	2:1	Dark red crystals	39
4	16	11.9			100	2:1	Dark red crystals	31
5	14.7	11			100	2:1	Dark red crystals	34
6	15.3	11.5			100	2:1	Dark red crystals	31
7	14.7	11	2.9		100	2:1	Dark red crystals	29
8	15.3	11.5		HCl	100	2:1	PXRD H_4pdi linker	-
9	15.7	11.6		TFA	100	2:1	Dark red crystals	34
10	16.1	12.1		HAc	100	2:1	Dark red crystals	40
11	18.8	14			100	2:1	Dark red crystals	59
12	15.7	11.8			100	2.1	Dark red crystals	47

13	18.8	14.1			100	2:1	Dark red crystals	67
14	17.5	15			120	2:1	Dark red crystals	72
15	17.5	15	3.3		120	2:1	Dark red crystals	59
16	21	18			120	2:1	Dark red crystals	57
17	20.3	17.5			120	2:1	Dark red crystals	58
Metal salt: $Zn(NO_3)_2 \cdot 6\ H_2O$								
Sample	**Metal salt [mg]**	**H_2pdb [mg]**	**DABCO [mg]**	**Acid (20 µL)**	**Temperature [°C]**	**Molar M:L ratio**	**Results**	**Yields [%]**
1	17	25			100	1:1	PXRD H_2pdb linker	-
2	34	25			100	2:1	PXRD H_2pdb linker	-
3	51	25			100	3:1	PXRD H_2pdb linker	-
4	13	50			100	1:2	PXRD H_2pdb linker	-
5	13	75			100	1:3	PXRD H_2pdb linker	-
6	6.8	20			120	1:2	PXRD H_2pdb linker	-
7	6.8	20		HCl	120	1:2	PXRD H_2pdb linker	-
8	6.8	20		HAc	120	1:2	PXRD H_2pdb linker	-
9	3.4	10		TFA	120	1:2	PXRD H_2pdb linker	-
10	6.8	30			120	1:3	PXRD H_2pdb linker	-
11	6.8	30		HCl	120	1:3	PXRD H_2pdb linker	-
12	6.8	30		HAc	120	1:3	PXRD H_2pdb linker	-
13	6.8	30		TFA	120	1:3	PXRD H_2pdb linker	-
14	3.4	15	1.3		120	1:3	PXRD H_2pdb linker	-
15	3.4	15	1.3	HCl	120	1:3	PXRD H_2pdb linker	-
16	3.4	15	1.3	HAc	80	1:3	Yellow crystals[1]	36
17	4.2	15.2	1.6	HAc	80	1:3	Yellow crystals[1]	34
18	7.4	30.5	3.0	HAc	80	1:3	Yellow crystals[1]	38
19	3.4	15	1.3	TFA	120	1:3	PXRD H_2pdb linker	-
Metal salt: $Zn(NO_3)_2 \cdot 6\ H_2O$								
Sample	**Metal salt [mg]**	**H_4pdi [mg]**	**DABCO [mg]**	**Acid (20 µL)**	**Temperature [°C]**	**M:L ratio**	**Results**	**Yields [%]**
1	17.5	15			120	2:1	Dark yellow crystals	45
2	17.5	15	3.3		120	2:1	Dark yellow crystals	40
3	21	18			120	2:1	Dark yellow crystals	38
4	20.3	17.5			120	2:1	Dark yellow crystals	37
Metal salt: $ZrCl_4$								
Sample	**Metal salt [mg]**	**H_2pdb [mg]**	**DABCO [mg]**	**Acid (20 µL)**	**Temperature [°C]**	**Molar M:L ratio**	**Results**	**Yields [%]**
1	13.3	25			100	1:1	PXRD H_2pdb linker	-
2	26.6	25			100	2:1	Amorphous solid	60
3	39.9	25			100	3:1	Amorphous solid	68
4	13.3	50			100	1:2	Amorphous solid	50
5	13.3	75			100	1:3	Amorphous solid	55
6	5.3	20			120	1:2	Amorphous solid	54
7	5.3	20		HCl	120	1:2	Amorphous solid	49
8	5.3	20		HAc	120	1:2	PXRD H_2pdb linker	-
9	2.7	10		TFA	120	1:2	Amorphous solid	61

10	5.3	30			120	1:3	Amorphous solid	49
11	5.3	30		HCl	120	1:3	Amorphous solid	45
12	5.3	30		HAc	120	1:3	Amorphous solid	46
13	5.3	30		TFA	120	1:3	Amorphous solid	39
Metal salt: $ZrOCl_2 \cdot 8\ H_2O$								
Sample	**Metal salt [mg]**	**H_2pdb [mg]**	**DABCO [mg]**	**Acid (20 µL)**	**Temperature [°C]**	**Molar M:L ratio**	**Results**	**Yields [%]**
1	18	25			100	1:1	Amorphous solid	58
2	36	25			100	2:1	Amorphous solid	49
3	54	25			100	3:1	Amorphous solid	61
4	18	50			100	1:2	Amorphous solid	55
5	18	75			100	1:3	Amorphous solid	51
6	7.4	20			120	1:2	Amorphous solid	54
7	7.4	20		HCl	120	1:2	Amorphous solid	49
8	7.4	20		HAc	120	1:2	Amorphous solid	42
9	3.7	10		TFA	120	1:2	Amorphous solid	42
10	7.4	30			120	1:3	Amorphous solid	47
11	7.4	30		HCl	120	1:3	Amorphous solid	51
12	7.4	30		HAc	120	1:3	Amorphous solid	50
13	7.4	30		TFA	120	1:3	Amorphous solid	48
Metal salt: $AlCl_3 \cdot 6\ H_2O$								
Sample	**Metal salt [mg]**	**H_2pdb [mg]**	**DABCO [mg]**	**Acid (20 µL)**	**Temperature [°C]**	**Molar M:L ratio**	**Results**	**Yields [%]**
1	5.5	20			120	1:2	Amorphous solid	60
2	5.5	20		HCl	120	1:2	Amorphous solid	57
3	5.5	20		HAc	120	1:2	Amorphous solid	59
4	2.6	10		TFA	120	1:2	Amorphous solid	49
5	5.5	30			120	1:3	Amorphous solid	48
6	5.5	30		HCl	120	1:3	Amorphous solid	48
7	5.5	30		HAc	120	1:3	Amorphous solid	46
8	5.5	30		TFA	120	1:3	Amorphous solid	48
Metal salt: $NiSO_4 \cdot 6\ H_2O$								
Sample	**Metal salt [mg]**	**H_2pdb [mg]**	**DABCO [mg]**	**Acid (20 µL)**	**Temperature [°C]**	**Molar M:L ratio**	**Results**	**Yields [%]**
1	3	15		TFA	120	1:3	PXRD H_2pdb linker	-
Metal salt: $Ni(NO_3)_2$								
Sample	**Metal salt [mg]**	**H_2pdb [mg]**	**DABCO [mg]**	**Acid (20 µL)**	**Temperature [°C]**	**Molar M:L ratio**	**Results**	**Yields [%]**
1	16.6	25			100	1:1	PXRD H_2pdb linker	-
2	33.2	25			100	2:1	PXRD H_2pdb linker	-
3	49.8	25			100	3:1	PXRD H_2pdb linker	-
4	16.6	50			100	1:2	PXRD H_2pdb linker	-
5	16.6	75			100	1:3	PXRD H_2pdb linker	-
6	6.7	20			120	1:2	PXRD H_2pdb linker	-
7	6.7	20		HCl	120	1:2	PXRD H_2pdb linker	-
8	6.7	20		HAc	120	1:2	PXRD H_2pdb linker	-
9	1.6	10		TFA	120	1:4	Light yellow solid	40
Metal salt: $NiCl_2 \cdot 6\ H_2O$								

Sample	Metal salt [mg]	H_2pdb [mg]	DABCO [mg]	Acid (20 µL)	Temperature [°C]	Molar M:L ratio	Results	Yields [%]
1	5.4	20		TFA	120	1:2	PXRD H_2pdb linker	-
2	5.4	30		HCl	120	1:3	PXRD H_2pdb linker	-
3	5.4	30		HAc	120	1:3	PXRD H_2pdb linker	-
4	5.4	30		TFA	120	1:3	PXRD H_2pdb linker	-
5	5.4	30			120	1:3	PXRD H_2pdb linker	-
Metal salt: $CuCl_2 \cdot H_2O$								
Sample	**Metal salt [mg]**	**H_2pdb [mg]**	**DABCO [mg]**	**Acid (20 µL)**	**Temperature [°C]**	**Molar M:L ratio**	**Results**	**Yields [%]**
1	3	20			120	1:2	PXRD H_2pdb linker	-
2	3	20		HCl	120	1:2	PXRD H_2pdb linker	-
3	3	20		HAc	120	1:2	PXRD H_2pdb linker	-
4	1.5	10		TFA	120	1:2	PXRD H_2pdb linker	-
5	3.1	30			120	1:3	PXRD H_2pdb linker	-
6	3.1	30		HCl	120	1:3	PXRD H_2pdb linker	-
7	3.1	30		HAc	120	1:3	PXRD H_2pdb linker	-
8	3.1	30		TFA	120	1:3	PXRD H_2pdb linker	-

Results with “PXRD H_2pdb linker” or with "PXRD H_4pdi linker" mean that the measured PXRD shows the same reflections as the pure linker and no reflections were measured for “amorphous solid.” The PXRD pattern which shows only reflections of the free linker indicates that no crystalline coordination polymer was formed under these conditions and that the linker recrystallized from the reaction mixture. The absence of reflections of the metal salt is attributed to the fact that the metal precursor remained dissolved as solvated species in the mother liquor (and/or in an amorphous form), which is not detectable by PXRD. Powder diffraction therefore only reflects the crystalline solid phase present after the reaction, namely the unreacted linker.

3 mL of DMF (*N,N*-dimethylformamide) was used in each reaction. Used acids: HCl = hydrochloric acid (c = 12 mol/L); HAc = acetic acid (neat); TFA = trifluoroacetic acid (neat).

When DABCO was used in the syntheses, a molar ratio of 1 relative to the linker was used.

Some approaches were repeated for reproduction purposes.

In some experiments, different acids were tested as modulators. Acidic modulators have been reported in the literature for the synthesis of such coordination polymers (especially MOFs), as they influence nucleation and crystallization kinetics and, through competitive coordination to the metal centers, can control framework formation and defect generation. The variation referred to the identity of the acid in order to examine how differences in coordination strength and steric properties affect framework assembly.

Section S6 Crystal photographs and crystal structure images

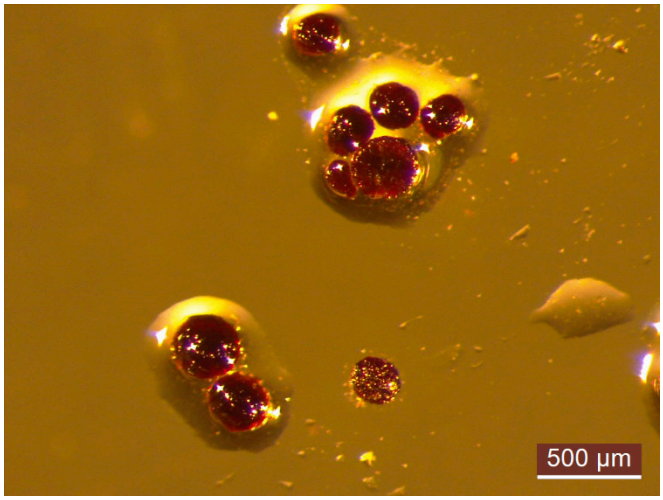


Figure S12. Light microscope photograph of [Co(pdb)(DMF)].

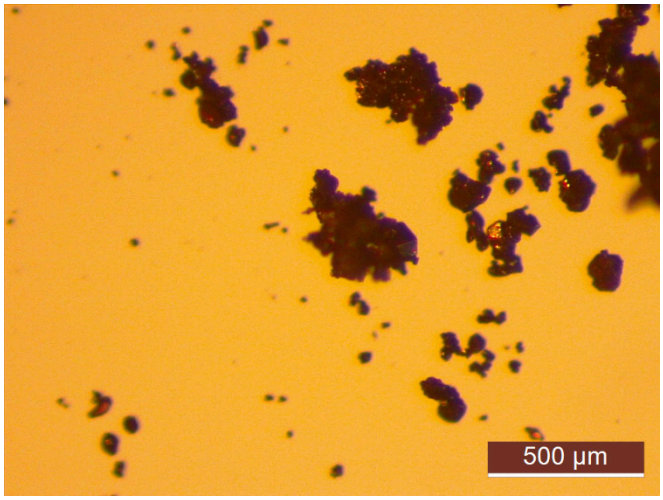


Figure S13. Light microscope photograph of $[Co_2(pdi)(DMF)_3]\cdot 2(DMF)\cdot H_2O$.

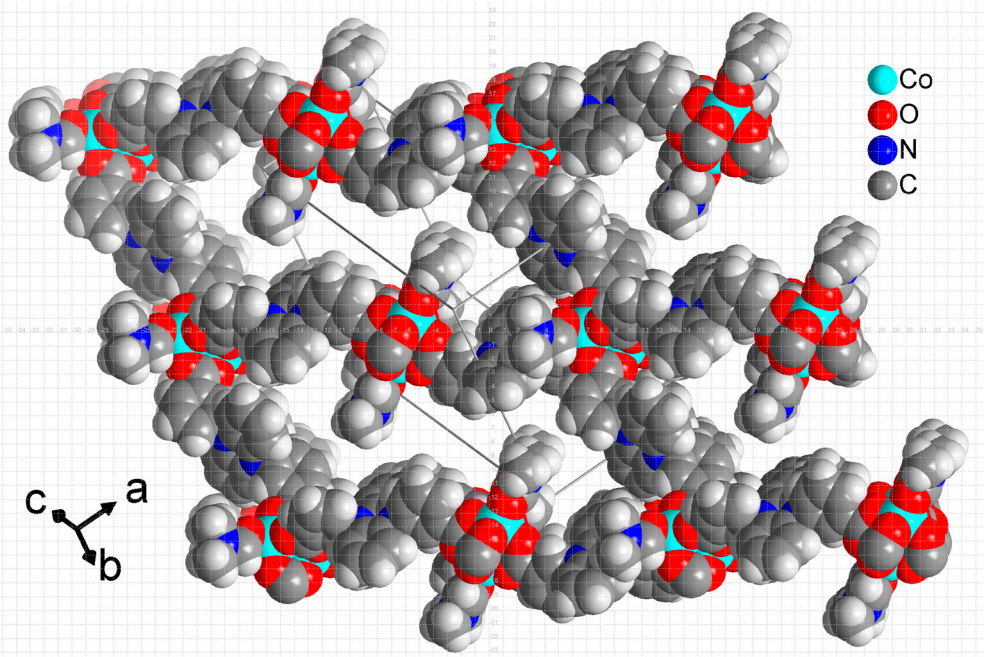


Figure S14. Space-filling view of the [Co(pdb)(DMF)] network with hydrogen atoms included. The edges of the square in the underyling grid are 1 Å.

Section S7 PXRD

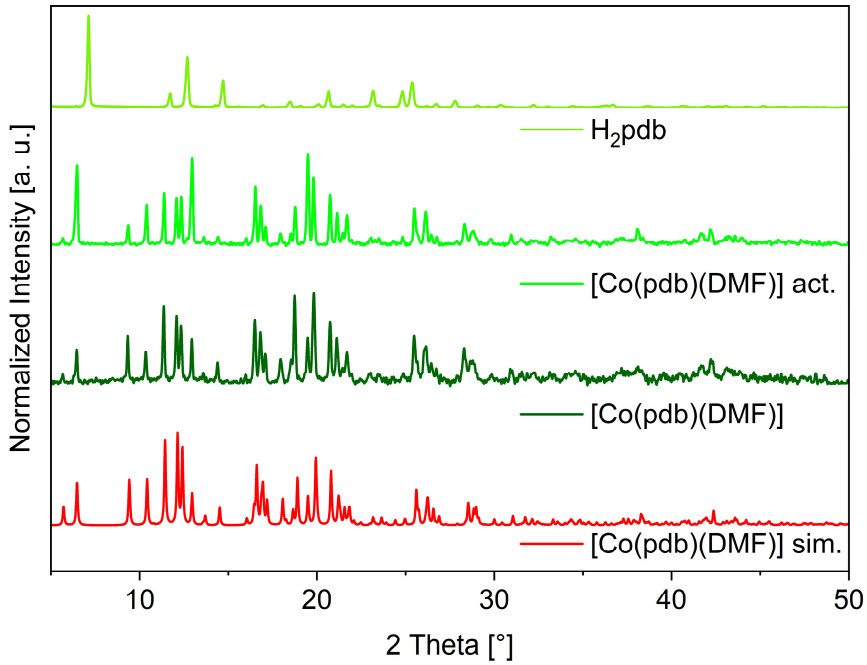


Figure S15. Powder X-ray diffraction pattern of dimethyl-3,3'-(phenazine-5,10-diyl)dibenzoate (H_2pdb) (yellow-green), simulated (sim.) (red) and experimental powder X-ray diffraction patterns of [Co(pdb)(DMF)] before (olive green) and after activation (light green). Activation was done on the pre-dried sample (12 h at 60 °C under vacuum) for 3 h at 130 °C under turbomolecular pump vacuum ($5 \cdot 10^{-12}$ bar).

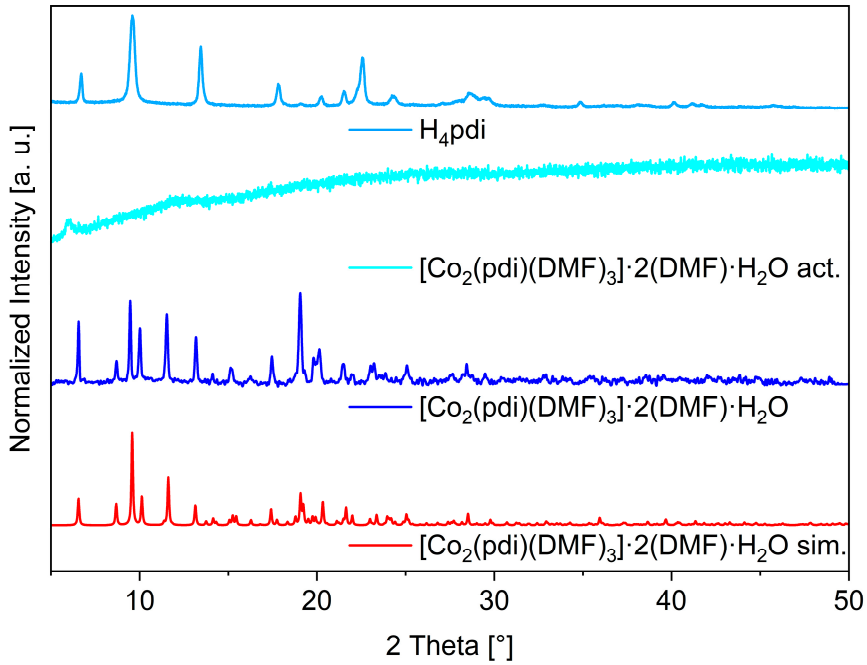
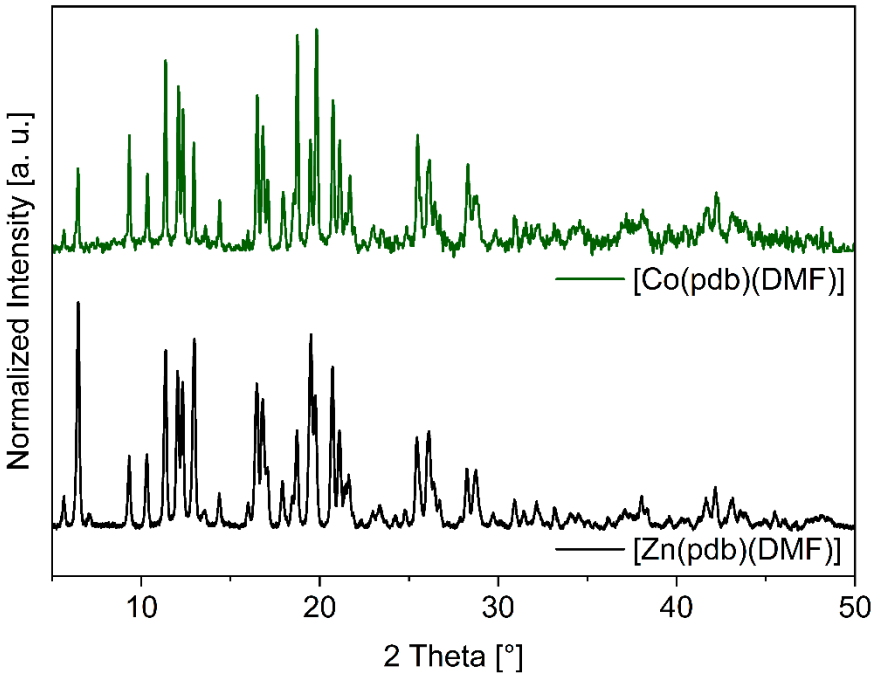
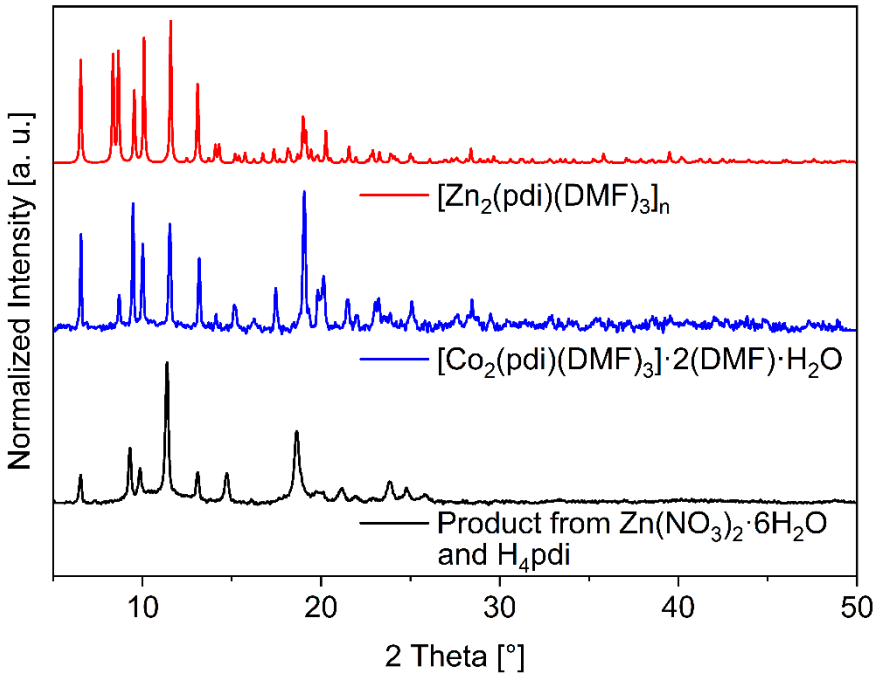


Figure S16. Powder X-ray diffraction pattern of 5,5'-(phenazine-5,10-diyl)diisophthalic acid (H_4pdi) (light blue), simulated (sim.) (red) and experimental powder X-ray diffraction patterns of $[Co_2(pdi)(DMF)_3]\cdot 2(DMF)\cdot H_2O$ before (dark blue) and after acitvation (cyan). Activation was done on the pre-dried sample (12 h at 60 °C under vacuum) for 3 h at 130 °C under turbomolecular pump vacuum ($5 \cdot 10^{-12}$ bar). Also, milder activation conditions (16 h at 60 °C under vacuum) yielded an amorphous product with a featureless PXRD pattern.



a)



b)

Figure S17. (a) Powder X-ray diffraction patterns of [Co(pdb)(DMF)] (olive green) and the isostructural zinc complex from the reaction of $Zn(NO_3)_2 \cdot 6\ H_2O$ and H_2pdb (black); (b) Powder X-ray diffraction patterns of $[Co_2(pdi)(DMF)_3] \cdot 2(DMF) \cdot H_2O$ (blue), the isostructural zinc complex from the reaction of $Zn(NO_3)_2 \cdot 6\ H_2O$ and H_4pdi (black) and isostructural $[Zn_2(pdi)(DMF)_3]_n$ (red) from the literature (where the linker is denoted as PDPA) [1]. The crystal solvent in the publication of the 298 K structure of $[Zn_2(pdi)(DMF)_3]_n$ had been omitted and was not refined.

The experimental PXRD of [Co(pdb)(DMF)] and the resulting zinc complex showed a matching pattern with reflections at the same 2θ angles and of similar intensity (Figure S17a) which verified that the structures are isostructural with each other.

Section S8 Thermogravimetric analyses

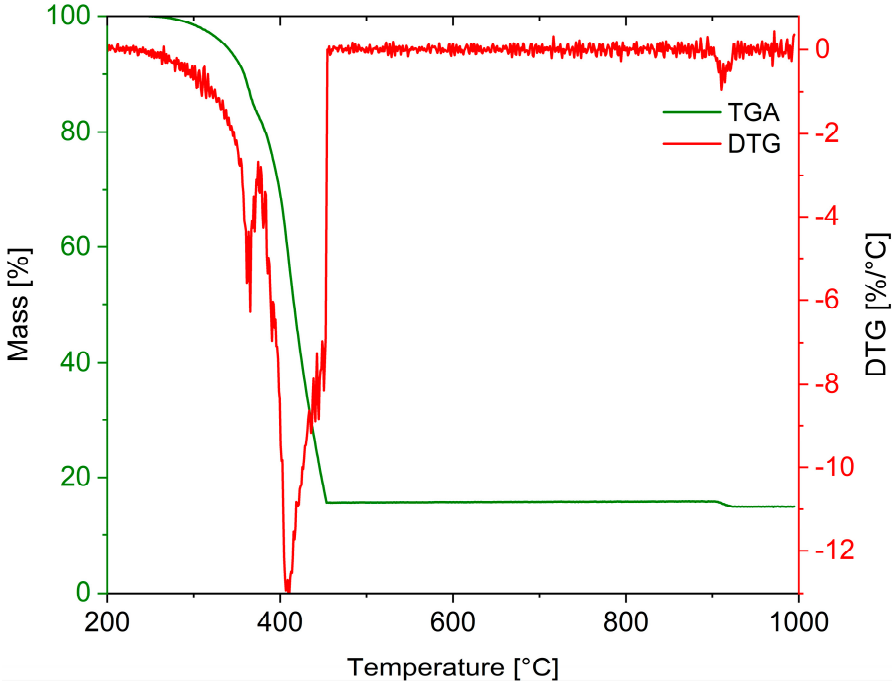


Figure S18. TGA and DTG of [Co(pdb)(DMF)] under synthetic air after drying for 14 h at 180 °C and handling under vacuum (10^{-3} bar), heating rate 10 K min^{-1}. The minor mass decrease observed at temperatures above ~900 °C can be attributed to the thermal transformation of cobalt(II,III) oxide, Co_2O_3 to cobalt(II) oxide, CoO, which is known to occur at elevated temperatures and would correspond to only a small mass change [2].

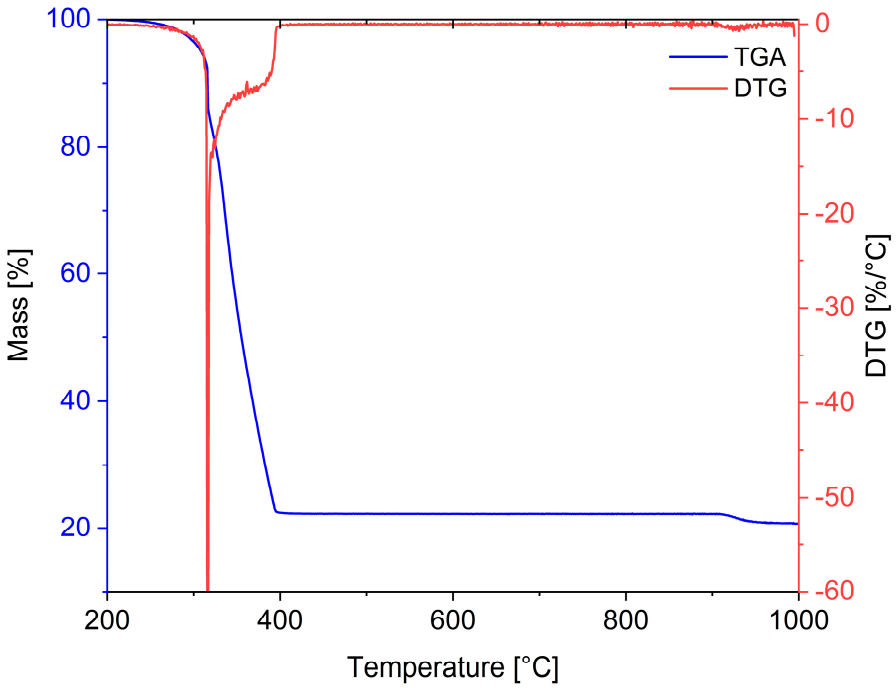


Figure S19. TGA and DTG of $[Co_2(pdi)(DMF)_3]\cdot 2(DMF)\cdot H_2O$ under synthetic air after drying for 14 h at 180 °C under vacuum (10^{-3} bar), heating rate 10 K min^{-1}. The minor mass decrease observed at temperatures above ~900 °C can be attributed to the thermal transformation of cobalt(II,III) oxide, Co_2O_3 to cobalt(II) oxide, CoO, which is known to occur at elevated temperatures and would correspond to only a small mass change [2].

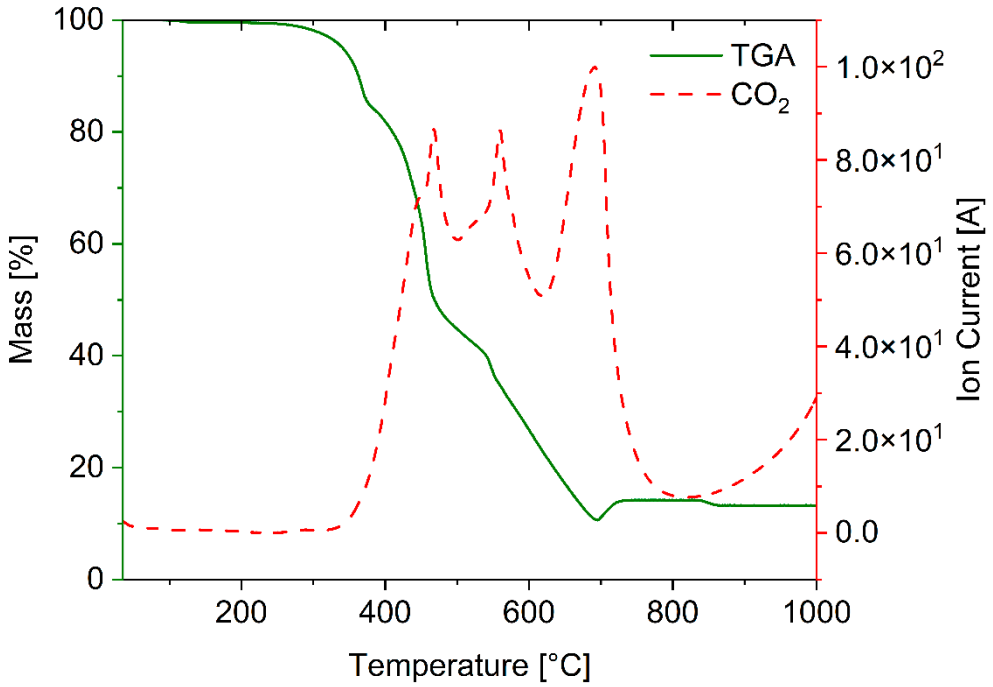


Figure S20. TGA coupled with mass spectrometry, TG-MS of [Co(pdb)(DMF)] (carried out under nitrogen, heating rate 10 K min^{-1}). The sample was dried for 14 h at 180 °C under vacuum (10^{-3} bar).

The coupled TGA–MS measurement of [Co(pdb)(DMF)] under nitrogen reveals a framework decomposition dominated by decarboxylation and subsequent carbonization. Below 200 °C, only a negligible mass loss is observed and no CO_2 evolution is detected, indicating the absence of significant solvent release or linker degradation. The onset of decomposition occurs at approximately 300-350 °C, followed by a first sharp and then more gradual mass-loss between ca. 420 and 690 °C, which coincides with CO_2 evolution from decarboxylation and is assigned to the decomposition of the organic linker. Above ~750-800 °C, gas evolution ceases and a stable cobalt-oxide residue remains with 14-15 wt%, consistent with the formation of cobalt oxide CoO (theor. 14 wt% for CoO, 15 wt% for Co_2O_3, 11 wt% for Co). Although the measurement was carried out under nitrogen, cobalt oxide species can form due to oxygen originating from the carboxylate groups (internal oxygen source) during thermal decomposition. On the other hand, the dip in mass% at 700 °C is probably due to the initial formation of cobalt metal under the nitrogen atmosphere which then forms cobalt oxide by reacting with oxygen impurities in the nitrogen purge gas giving the mass% gain with increasing temperature.

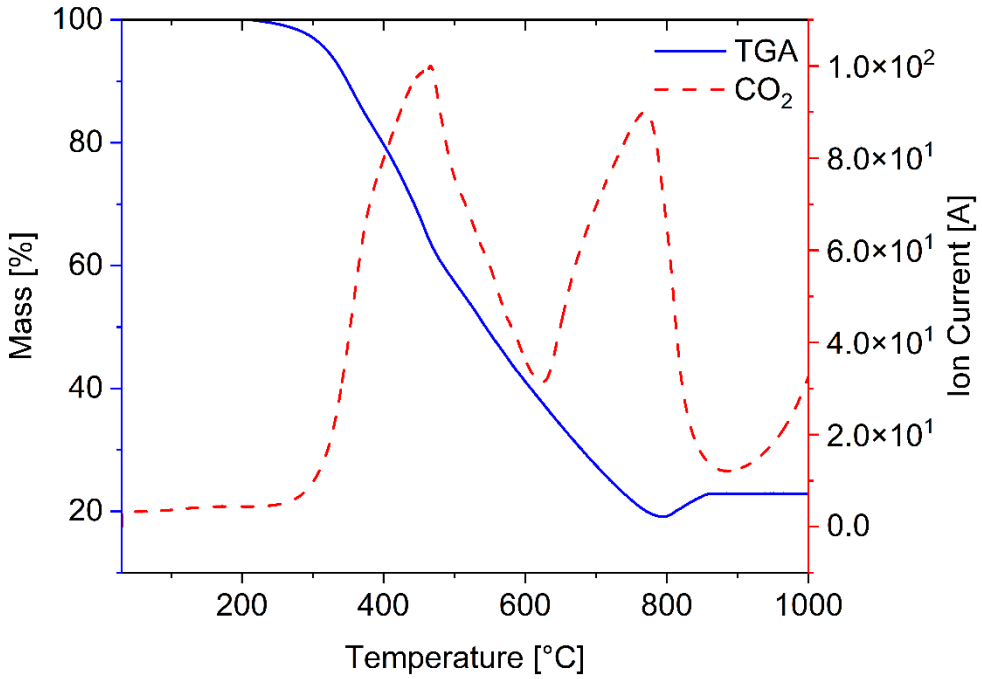


Figure S21. TGA coupled with mass spectrometry, TG-MS of $[Co_2(pdi)(DMF)_3]\cdot 2(DMF)\cdot H_2O$ (carried out under nitrogen, heating rate 10 K min^{-1}). The sample was dried for 14 h at 180 °C under vacuum (10^{-3} bar).

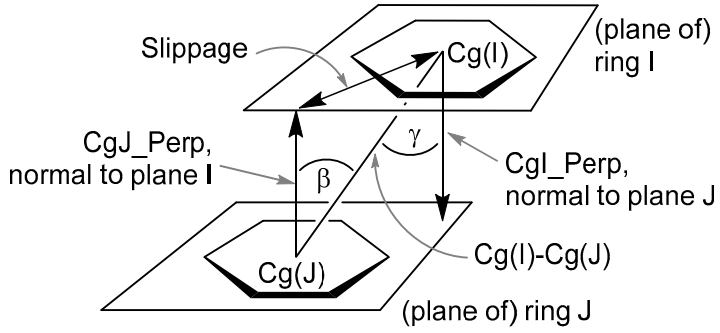
The coupled TGA-MS analysis of $[Co_2(pdi)(DMF)_3]$ starts with the first mass loss at ~300 °C due to the loss of the coordinated DMF (theor. 26 wt%) and continues without a plateau to ~790 °C with degradation of the organic linker (theor. 60 wt%). A concomitant CO_2 evolution from decarboxylation underscores the decomposition of the organic linker. At 1000 °C, a residue of 21 wt% remains (theor. 18 wt%, 20 wt% for Co_2O_3, 14 wt% for Co) which may also include a carbonaceous matrix still present under the nitrogen atmosphere. The dip in mass% at just below 800 °C is probably due to the initial formation of cobalt metal under the nitrogen atmosphere which then forms cobalt oxide by reacting with oxygen impurities in the nitrogen purge gas giving the mass% gain with increasing temperature.

Section S9 Supramolecular analyses

The supramolecular analyses for possible π–π, C–H-π and C–H···O interactions was carried out with the program PLATON [3]

a) Analysis for compound [Co(pdb)(DMF)]

The PLATON-listing "Analysis of Short Ring-Interactions" for possible π-stacking interactions yielded a single long π-stacking contact for [Co(pdb)(DMF)].
For comparison, "strong" π-stacking interactions have rather short centroid-centroid contacts (<3.8 Å), near parallel ring planes (alpha < 10° to ~0° or even exactly 0° by symmetry), small slip angles (β, γ <25°) and vertical displacements (slippage <1.5 Å) which translate into a sizable overlap of the aryl-plane areas (Scheme S6, Table S3, Figure S22) [4,5].



Scheme S6. Graphical presentation of the parameters used for the description of π-π stacking.

Table S3. Packing analysis for possible π-stacking interactions in [Co(pdb)(DMF)].

==========

Analysis of short ring-interactions with Cg-Cg distances < 4.0 Ang., Alpha < 20.000 Deg. and Beta < 60.0 Deg.

==========

- Cg(I) = Plane number I (= ring number in () above)
- Alpha = Dihedral Angle between Planes I and J (Deg)
- Beta = Angle Cg(I)-->Cg(J) or Cg(I)-->Me vector and normal to plane I (Deg)
- Gamma = Angle Cg(I)-->Cg(J) vector and normal to plane J (Deg)
- Cg-Cg = Distance between ring Centroids (Ang.)
- CgI_Perp = Perpendicular distance of Cg(I) on ring J (Ang.)
- CgJ_Perp = Perpendicular distance of Cg(J) on ring I (Ang.)
- Slippage = Distance between Cg(I) and Perpendicular Projection of Cg(J) on Ring I (Ang).

Cg(I)	Cg(J)	[ARU(J)]	Cg-Cg	Alpha	Beta	Gamma	CgI_Perp	CgJ_Perp	Slippage
Cg5	Cg5	[2456.01]	3.966(3)	16.5(2)	17.5	17.5	3.782(2)	3.782(2)	1.195

[2456] = iv = -1/2-X, Y, 1-Z

Cg5 = centroid of ring C14-C15-C16-C17-C18-C19

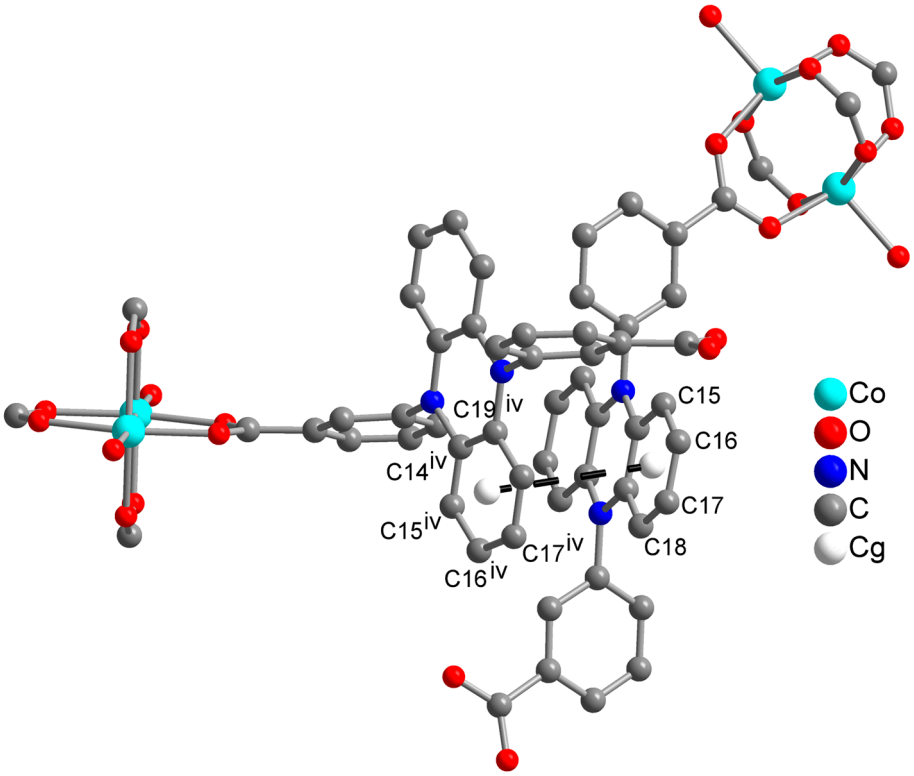
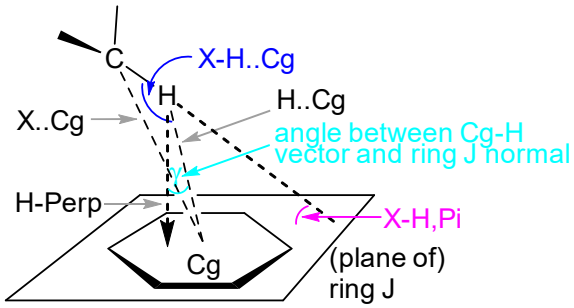


Figure S22. π-π interactions in the packing of [Co(pdb)(DMF)] in the crystal, indicated as a dashed black line with the centroid-centroid contact of 3.966 Å. Further details of this π-π interaction, are listed in the above Table S3 (Cg = ring centroid). Symmetry transformation iv = -1/2-X, Y, 1-Z.

Limited C-H···π contacts were found for [Co(pdb)(DMF)].

Significant intermolecular C-H···π contacts start below around 2.7 Å for the (C-)H···ring centroid distances with H-perp also starting at below 2.6-2.7 Å and C-H··Cg > 145° (Scheme S7, Table S4, Figure S23 [6,7].



Scheme S7. Graphical presentation of the parameters used for the description of CH-π interactions.

Table S4. Analysis of *inter*molecular C–H...Cg(pi-ring) interactions (H..Cg < 3.0 Ang. - Gamma < 30.0 Deg) in [Co(pdb)(DMF)].

- Cg(J) = Center of gravity of ring J (Plane number above)

- H-Perp = Perpendicular distance of H to ring plane J

- Gamma = Angle between Cg-H vector and ring J normal

- X-H..Cg = X-H-Cg angle (degrees)

- X..Cg = Distance of X to Cg (Angstrom)

- X-H, Pi = Angle of the X-H bond with the Pi-plane (i.e.' Perpendicular = 90 degrees, Parallel = 0 degrees)

C--H(I)	Cg(J)	[ARU(J)]	H..Cg	H-Perp	Gamma	X-H..Cg	X..Cg	X-H,Pi
C9 -H9	Cg3	[4475.01]	2.72	2.53	22	150	3.571(8)	78
C21 -H21	Cg5	[4465.01]	2.83	2.69	18	137	3.565(9)	4

[4475] = v = -1/2+X, 2-Y, Z

[4465] = vi = -1/2+X, 1-Y, Z

Cg3 = centroid of ring C1-C2-C3-C4-C5-C6

Cg5 = centroid of ring C14-C15-C16-C17-C18-C19

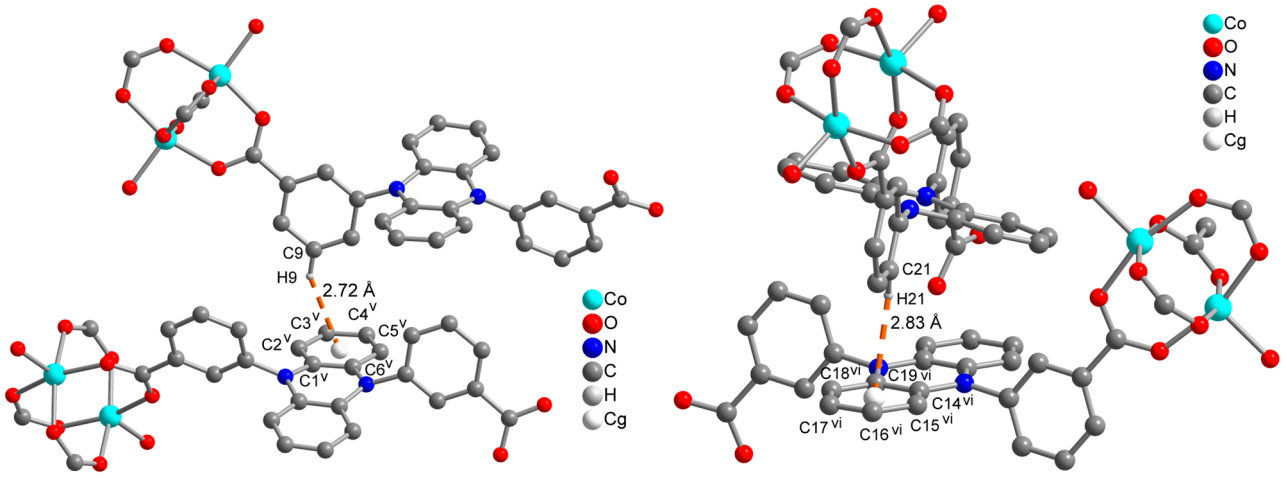


Figure S23. C-H···π interactions in the packing of [Co(pdb)(DMF)] in the crystal, indicated as dashed orange lines with the H-centroid distance. Further details of these C-H···π interactions are listed in the above Table S4 (Cg = ring centroid). Symmetry transformations v = -1/2+X, 2-Y, Z, vi = -1/2+X, 1-Y, Z.

Table S5. Packing analysis for possible C–H···O interactions in [Co(pdb)(DMF)].

==========

Analysis of Potential Hydrogen Bonds and Schemes with d(D...A) < R(D)+R(A)+0.50, d(H...A) < R(H)+R(A)-0.12 Ang., D-H...A > 100.0 Deg

==========

Note: - ARU codes in [] are with reference to the Coordinates printed above (Possibly transformed, when MOVE /= 1.555)

==========

Donor --- H....Acceptor [ARU]	D - H	H...A	D...A	D - H...A
C3 --H3 O4 [1655.01]	0.95	2.57	3.377(6)	143
C27 --H27 O4 [7566.01]	0.95	2.50	3.122(6)	123

C28	--H28A	O3	[4565.01]	0.98	2.57	3.257(6)	127

[7566.] = [7_566] = i = 1/2-x, 3/2-y, 3/2-z

[4565.] = [6_665] = vii = 1/2+x, 1-y, z

[1655.] = [1_655] = viii = 1+x, y, z

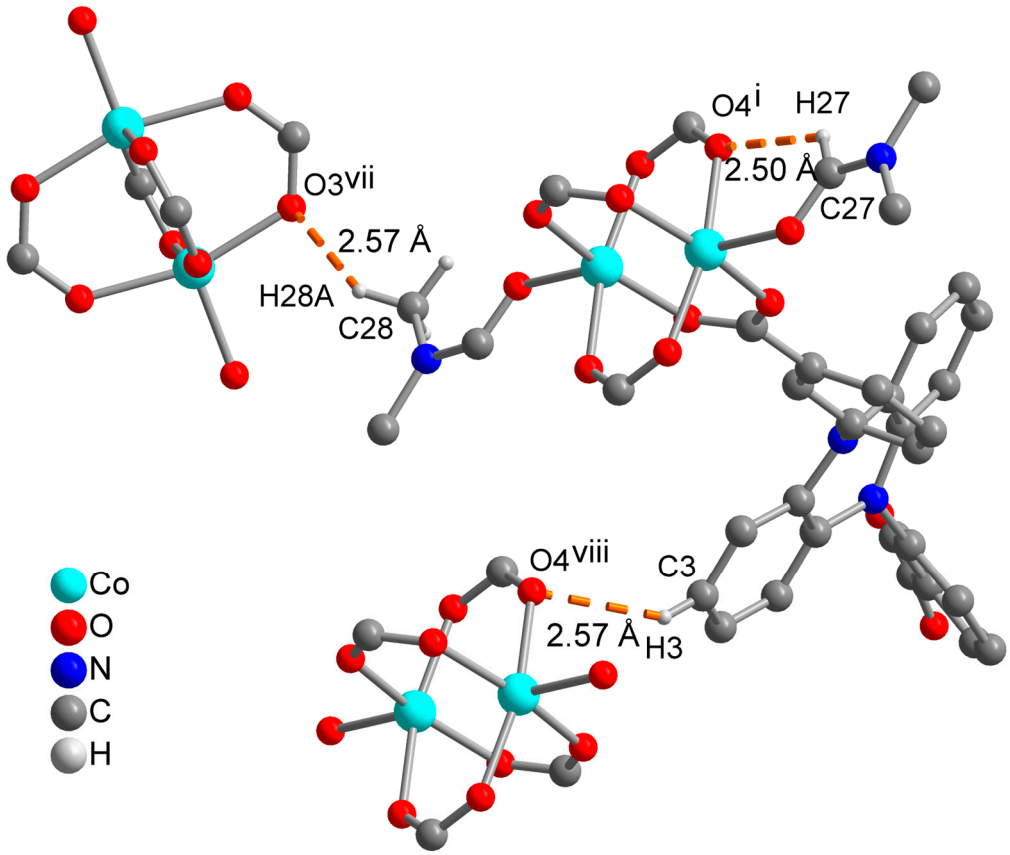


Figure S24. C-H···O contacts in the packing of [Co(pdb)(DMF)] in the crystal, indicated as dashed orange lines with the H···O distances. Further details of these C-H···O interactions, including the symmetry transformations are listed in the above Table S5.

b) Analysis for compound $[Co_2(pdi)(DMF)_3]\cdot 2(DMF)\cdot H_2O$

See also the general comments on the distances and angles of π–π and C–H-π interactions given in the analysis for compound [Co(pdb)(DMF)]

The PLATON-listing "Analysis of Short Ring-Interactions" for possible π-stacking interactions yielded no π-stacking contact with a centroid-centroid distance of less than 4.0 Å for $[Co_2(pdi)(DMF)_3]\cdot 2(DMF)\cdot H_2O$. The shortest centroid-centroid distance was 4.78 Å.

Also, limited C-H···π contacts were found for $[Co_2(pdi)(DMF)_3]\cdot 2(DMF)\cdot H_2O$.

Table S6. Analysis of *inter*molecular C–H...Cg(pi-ring) interactions (H..Cg < 3.0 Ang. - Gamma < 30.0 Deg) in $[Co_2(pdi)(DMF)_3]\cdot 2(DMF)\cdot H_2O$.

- Cg(J) = Center of gravity of ring J (Plane number above)
- H-Perp = Perpendicular distance of H to ring plane J
- Gamma = Angle between Cg-H vector and ring J normal
- X-H..Cg = X-H-Cg angle (degrees)
- X..Cg = Distance of X to Cg (Angstrom)
- X-H, Pi = Angle of the X-H bond with the Pi-plane (i.e.' Perpendicular = 90 degrees, Parallel = 0 degrees)

C--H(I)	Cg(J)	[ARU(J)]	H..Cg	H-Perp	Gamma	X-H..Cg	X..Cg	X-H,Pi
C36 -H36A	Cg11	[2664.01]	2.82	2.79	8.4	144	3.658(10)	51
C37 -H37A	Cg11	[4465.01]	2.96	2.80	19	130	3.668(10)	33
C41 -H41	Cg12	[1555.01]	2.88	2.85	7.7	149	3.726(10)	64

[2664] = ii = 1-X, 1-Y, -1/2+Z

[4465] = i = -1/2+X, 3/2-Y, Z

[1555] = X, Y, Z

Cg11 = centroid of ring C1-C2-C3-C4-C5-C6

Cg12 = centroid of ring C7-C8-C9-C10-C11-C12

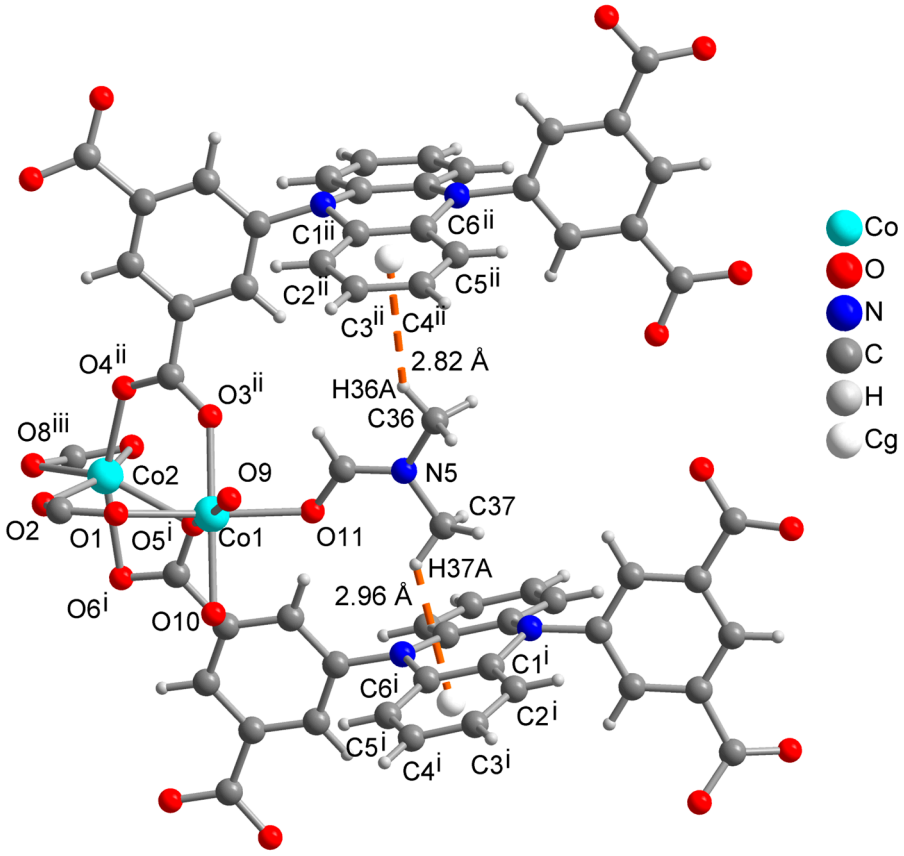


Figure S25. C-H···π interactions in the packing of $[Co_2(pdi)(DMF)_3]\cdot 2(DMF)\cdot H_2O$ in the crystal, indicated as dashed orange lines with the H-centroid distances. Further details of these C-H···π interactions are listed in the above Table S6 (Cg = ring centroid). Symmetry transformations i = $x-1/2$, $-y+3/2$, z; ii = $-x+1$, $-y+1$, $z-1/2$; iii = $-x+3/2$, $y+1/2$, $z-1/2$.

Table S7. Packing analysis for possible C–H···O interactions in $[Co_2(pdi)(DMF)_3]\cdot 2(DMF)\cdot H_2O$

==========

Analysis of Potential Hydrogen Bonds and Schemes with d(D...A) < R(D)+R(A)+0.50, d(H...A) < R(H)+R(A)-0.12 Ang., D-H...A > 100.0 Deg

==========

Note: - ARU codes in [] are with reference to the Coordinates printed above (Possibly transformed, when MOVE /= 1.555)

==========

Donor --- H....Acceptor	[ARU]	D - H	H...A	D...A	D - H...A
C14--H14 O14	[4565.04]	0.95	2.60	3.547(9)	175
C22--H22 O11	[4565.01]	0.95	2.42	3.300(6)	154
C29--H29 O3	[2664.01]	0.95	2.43	3.047(7)	122
C32--H32 O9	[ ]	0.95	2.55	3.130(9)	120
C33--H33B O12	[2675.02]	0.98	2.35	3.261(15)	154
C35--H35 O3	[2664.01]	0.95	2.49	3.028(6)	116
C36--H36B O14	[1555.04]	0.98	2.34	3.177(11)	143
C43--H43B O12	[1545.02]	0.98	2.53	3.483(14)	163

Note: the intramolecular C-H···O contacts within the DMF molecules, that is, from the CH_3 group to the aldehyde with acute C-H···O angles of less than 110° are not listed.

[2664.] = ii = 1-x, 1-y, -1/2+z

[4565.] = iv = 1/2+x, 3/2-y, z

[2675.] = v = 1-x, 2-y, 1/2+z

[1545.] = vi = x, -1+y, z

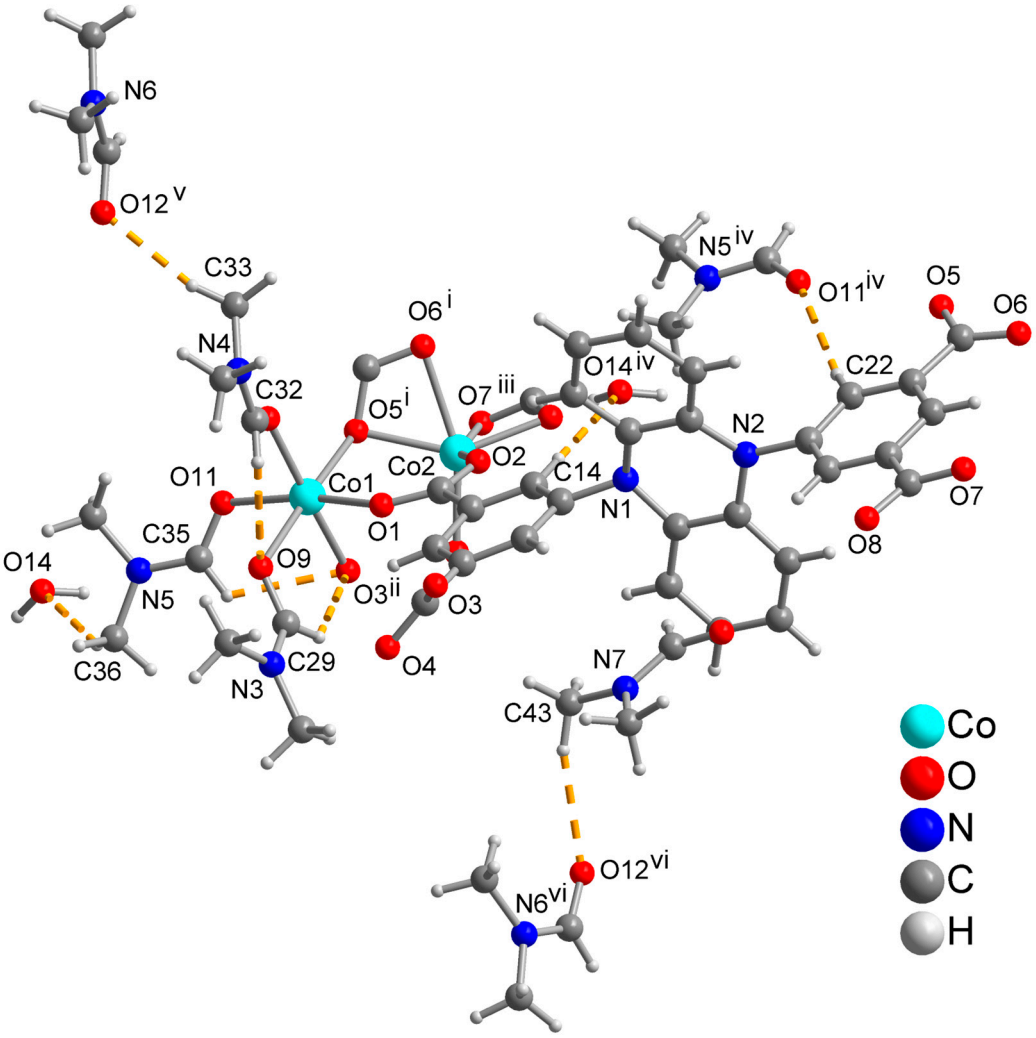
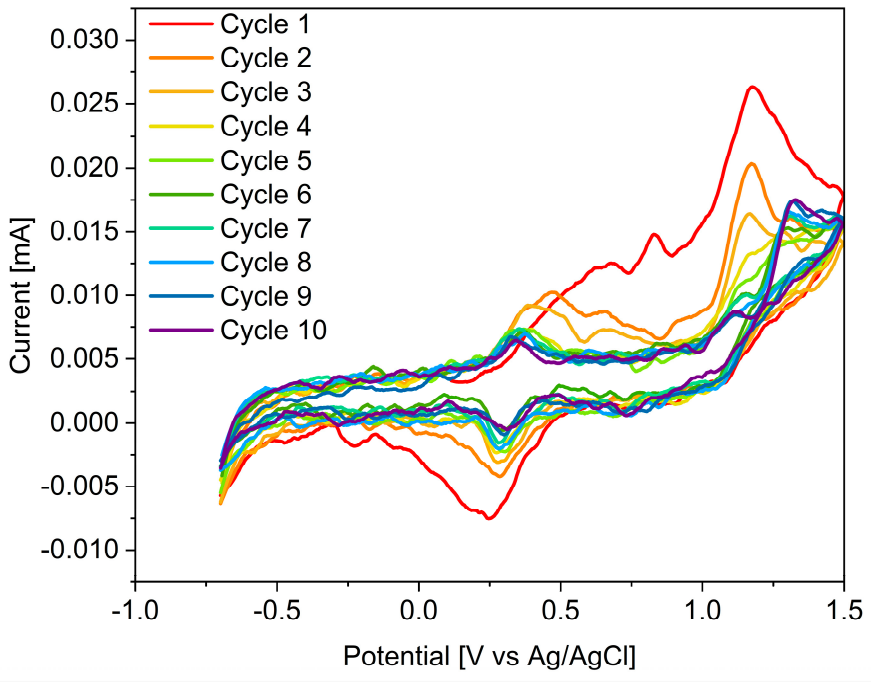
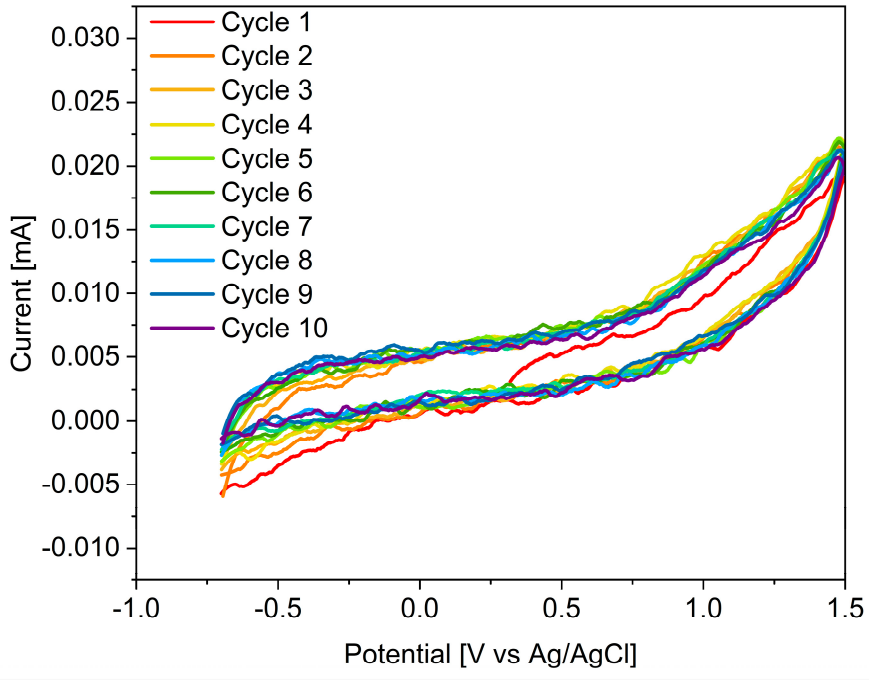


Figure S26. C-H···O contacts in the packing of $[Co_2(pdi)(DMF)_3]\cdot 2(DMF)\cdot H_2O$ in the crystal, indicated as dashed orange lines. Further details of these C-H···O interactions are listed in the above Table S7. Symmetry transformations i = *x*−1/2, -*y*+3/2, *z*; ii = −*x*+1, −*y*+1, *z*−1/2; iii = −*x*+3/2, *y*+1/2, *z*−1/2, iv = 1/2+x, 3/2-y, z; v = 1-x, 2-y, 1/2+z; vi = x, -1+y, z.

Section S10 Electrochemical measurements



a)



(b)

Figure S27. Cyclic voltammograms recorded over ten consecutive cycles for (a) [Co(pdb)(DMF)] and (b) $[Co_2(pdi)(DMF)_3]\cdot 2(DMF)\cdot H_2O$. In both cases, significant changes of the voltammetric response upon cycling or the absence of well-defined redox features are observed, indicating limited electrochemical stability and predominantly irreversible redox behavior.

1 Zhang, S.; Ma, X.-F.; Yang, Y.; Ren, H.; Li, W.; Liu, Y.; Xi, C.; Zheng, L.; Miao, Z. Phenazine-functionalized Zn-based metal organic framework for efficient visible light photocatalytic sulfides. *J. Solid State Chem.* **2025**, *351*, 125525. https://doi.org/10.1016/j.jssc.2025.125525.

2 Mandić, V.; Kurajica, S.; Plodinec, M.; Panžić, I. Thermal Stability and Utilization of 1D-Nanostructured Co_3O_4 Rods Derived by Simple Solvothermal Processing. *Catalysts* **2022**, *12* (10), 1162. https://doi.org/10.3390/catal12101162.

3 Spek, A. L. Structure Validation in Chemical Crystallography. *Acta Crystallogr. D* **2009**, *65*, 148–155. https://doi.org/10.1107/S090744490804362X.

4 Janiak, C. A Critical Account on π–π Stacking in Metal Complexes with Aromatic Nitrogen-Containing Ligands. J. Chem. *Soc., Dalton Trans.* **2000**, 3885–3896. https://doi.org/10.1039/b003010o.

5 Yang, X.-J.; Drepper, F.; Wu, B.; Sun, W.-H.; Haehnel, W.; Janiak, C. From Model Compounds to Protein Binding: Syntheses, Characterizations and Fluorescence Studies of $[Ru^{II}(Bipy)(Terpy)L]^{2+}$ Complexes (Bipy = 2,2′-Bipyridine; Terpy = 2,2′:6′,2″-Terpyridine; L = Imidazole, Pyrazole and Derivatives, Cytochrome c). *Dalton Trans.* **2005**, 256–267. https://doi.org/10.1039/B414999H.

6 Takahashi, O.; Kohno, Y.; Iwasaki, S.; Saito, K.; Iwaoka, M.; Tomoda, S.; Umezawa, Y.; Tsuboyama, S.; Nishio, M. Hydrogen-Bond-Like Nature of the CH/π Interaction as Evidenced by Crystallographic Database Analyses and Ab Initio Molecular Orbital Calculations, *Bull. Chem. Soc. Jpn.* **2001**, *74*, 2421–2430. https://doi.org/10.1246/bcsj.74.2421

7 Nishio, M.; Umezawa, Y.; Honda, K.; Tsuboyama, S.; Suezawa, H. CH/π Hydrogen Bonds in Organic and Organometallic Chemistry. *CrystEngComm* **2009**, *11*, 1757-1788. https://doi.org/10.1039/b902318f.